Homo- and heterodimerization of bHLH transcription factors balance stemness with bipotential differentiation in the *Drosophila* gut

Aleix Puig-Barbe[1,2], Svenja Dettmann[3,4], Vinicius Dias Nirello[5], Sina Azami[6], Bruce A. Edgar[7,8], Patrick Varga-Weisz[5,9], Jerome Korzelius[6,7,10] and Joaquín de Navascués[1,9,✉]

[1] European Cancer Stem Cell Research Institute, School of Biosciences, Cardiff University, Hadyn Ellis Building, Maindy Road, Cardiff CF24 4HQ, UK.

[2] Current address: EMBL-European Bioinformatics Institute, Wellcome Genome Campus, Hinxton, Cambridgeshire, CB10 1SD, UK.

[3] DKFZ/ZMBH Alliance, University of Heidelberg, Heidelberg, Germany.

[4] AbbVie Germany GmbH & Co. KG, Frankfurt, Germany.

[5] International Laboratory for Microbiome Host Epigenetics, Department of Genetics, Evolution, Microbiology, and Immunology, Institute of Biology, University of Campinas, Campinas, SP 13083-862, Brazil

[6] Max Planck Institute for Biology of Ageing, Joseph-Stelzmann-Straße 9B, 50931 Köln, Germany.

[7] DKFZ/ZMBH Alliance, University of Heidelberg, Heidelberg, Germany.

[8] Huntsman Cancer Institute & Dept. of Oncological Sciences, University of Utah, Salt Lake City, UT 84112, USA.

[9] School of Life Sciences, University of Essex, Wivenhoe Park, Colchester CO4 3SQ, UK.

[10] School of Biosciences, University of Kent, Canterbury, Kent, CT2 7NZ, UK.

✉ j.denavascues@essex.ac.uk

Running title: Da, Emc and Sc balance stemness and differentiation in the fly intestine

Key words: bHLH / stemness / differentiation / bipotent stem cell / intestinal stem cell

ABSTRACT

Multipotent adult stem cells must balance self-renewal with differentiation into various mature cell types. How this balance is regulated at the transcriptional level is poorly understood. Here we show that a network of basic Helix-Loop-Helix (bHLH) transcription factors controls both stemness and bi-potential differentiation in the *Drosophila* adult intestine. We find that homodimers of Daughterless (Da), homolog of mammalian E proteins, maintain the self-renewal of intestinal stem cells (ISCs), and antagonise the activity of heterodimers of Da and Scute (Sc), homolog of ASCL and a known regulator of intestinal secretory differentiation. The HLH factor Extramacrochaetae (Emc), homologous to Id proteins, promotes absorptive differentiation by titrating Da and Sc to. We further show that Emc prevents the committed absorptive progenitor (the enteroblast, EB) from de-differentiating, underscoring the plasticity of these cells. Switching physical interaction partners in this way enables the active maintenance of stemness while priming stem cells for differentiation along two alternative fates. Such regulatory logic could be recapitulated in other bipotent stem cell systems.

INTRODUCTION

The regulation of stem cell fate decisions hinges on transcriptional control by sequence-specific transcription factors (TFs). Central to this control is the formation of gene regulatory networks by TFs, whose activity and dynamics steer cells along particular differentiation trajectories (Graf and Enver, 2009; Levine and Davidson, 2005; Moris et al., 2016). These trajectories are often be construed as a succession of binary steps that are regulated by cross-antagonism between TF pairs (Graf and Enver, 2009; Simon et al., 2018). However, active multipotent stem cells need to decide between the maintenance of their stem identity and several options of commitment into distinct mature cell fates. To understand how multipotent stem cells make these choices, knowledge of the functional interactions between transcription factors is essential (Cinquin and Demongeot, 2005; 2002).

Intestinal stem cells (ISCs) are a paradigm of multipotency in adult tissues. In *Drosophila* and mammals, ISCs face a three-way choice between self-renewal and differentiation into either the secretory or absorptive cell lineage (reviewed in Crosnier et al., 2006; Jiang and Edgar, 2012; Philpott and Winton, 2014). The intestinal secretory lineage in *Drosophila* consists of enteroendocrine cells (EE), subclassified according to their peptide hormone secretion profiles (Guo et al., 2019b; Hung *et al*, 2020). Absorptive cells are mostly called enterocytes (ECs), which differ in morphology and function along the anterior-posterior axis of the gut (Buchon et al., 2013; Marianes and Spradling, 2013). In *Drosophila*, ISCs produce lineage-specific precursors through distinct molecular triggers. High Notch signalling induces formation of enteroblasts (EBs), which will give rise to ECs. Expression in ISCs of the bHLH (basic Helix-Loop-Helix) transcription factors Scute (Sc) or Asense (Ase), members of the *achaete-scute Complex* (*AS-C*, homologs of *ASCL* mammalian genes) induces the formation of EE precursors (pre-EEs), which quickly turn into mature EE cells (Bardin et al., 2010; Chen et al., 2018; Micchelli and Perrimon, 2006; Ohlstein and Spradling, 2006; Zeng and Hou, 2015). It is not clear whether upon ISC division, its daughter cells first commit to differentiation before choosing a lineage (two consecutive binary decisions), are already lineage-primed before they lose self-renewing ability (the same binary decisions in inverse order), or instead choose at the same time between self-renewal and two potential lineages to commit to (a three-way decision) (Perdigoto *et al*, 2011; Gervais and Bardin, 2017). Little is known about the molecular mechanisms that could allow a triple decision between self-renewal and bi-potential differentiation.

Transcription factors of the bHLH family control fate in multiple developmental contexts, from sex determination and mesoderm specification, to neurogenesis and immune cell type specification (reviewed in Bertrand et al., 2002; Murre, 2005; Murre et al., 1994). Their HLH motif mediates dimerization, while the preceding region, rich in basic amino acids, allows DNA binding (Massari and Murre, 2000). The class I of bHLH factors comprises proteins such as E47, E2-2 and HEB (E proteins, encoded by *TCF3/4/12* in mammals; *daughterless —da—* in *Drosophila*). Class I bHLH proteins can make dimers within their class (e.g. Da:Da, or E47:HEB), but also heterodimerise with class II bHLH factors. By contrast, class II bHLH factors such as MYOD or ASCL (MyoD and proteins encoded by genes of the *achaete/scute complex —AS-C—* in *Drosophila*) usually form trans-activating complexes only in heterodimers with class I factors (Murre et al., 1994). Both class I and class II factors can heterodimerise with class V proteins. The mammalian members of this class are named *Inhibitors of DNA binding* (Id proteins) because they lack the stretch of basic amino acids preceding the HLH domain, and this makes their heterodimers unable to bind DNA (Murre et al., 1994); their only homolog in *Drosophila* is *extra macrochaetae* (*emc*).

Class II bHLH factors are known to regulate differentiation in the metazoan intestine (reviewed in Hartenstein et al., 2017; Philpott and Winton, 2014). In *Drosophila*, Sc and Ase can initiate EE differentiation (Amcheslavsky et al., 2014; Bardin et al., 2010; Chen et al., 2018; Z. Guo and Ohlstein, 2015), while other bHLH genes maintain EE function (*dimmed*, homolog of *NeuroD*; Beebe et al., 2015), or promote their functional diversity (*tap*, homolog of *Neurogenin-3*; Hartenstein et al., 2017). On the other hand, Da is required for ISC maintenance, as ISCs mutant for *da* differentiate (Bardin et al., 2010; Lan et al., 2018). However, which interaction partners bind to Da to maintain stemness is not known, and how different bHLH factors dimerise to allow differentiation has not been explored. Here we identify the Da homodimer as the critical bHLH complex maintaining ISC self-renewal. In addition, we find a role of the HLH factor Emc in titrating Da and Sc to promote absorptive differentiation. We further find that Da:Da and Da:Sc dimers functionally cooperate in the promotion of ISC fate, but act antagonistically with respect to EE differentiation. Our results reveal a network of bHLH factors that forms a three-way switch to regulate self-renewal and bipotential differentiation in the adult fly gut.

RESULTS

emc is expressed preferentially in the absorptive lineage

As bHLH factors are essential for correct differentiation during adult intestinal homeostasis across metazoans, the *Drosophila* Id factor, *emc*, may have a regulatory function in the adult fly intestine, where it is strongly transcribed (Brown et al., 2014; Chintapalli et al., 2007; Dutta et al., 2015). We examined its expression pattern using the homozygous viable protein trap line $emc^{CPTI\text{-}002740}$ (Lowe et al., 2014) and detected Emc in all EBs (identified by their expression of a Notch responsive element, *GBE-Su(H)-lacZ*, from here on referred to as *NRE-lacZ*) and most ECs (identified by their nuclear size) in the posterior midgut (Fig 1A-C). EEs and ISCs, detected by their expression of the transcription factor Prospero (Pros) and the Notch ligand Delta (Dl), showed very low levels of expression or none (Fig 1C-E). This suggests *emc* expression may serve as marker for the absorptive lineage. This pattern of protein expression agreed with our analysis of two published single-cell RNAseq (scRNAseq) datasets (Hung *et al*, 2020; H. Li et al., 2022) comprising ~9800 cells (Fig S1A). We observe increased *emc* expression in EBs and ECs (Fig 1F) with a similar level of enrichment (compared to EEs and ISCs) to published markers of the absorptive lineage, such as *myoIA* (Fig 1G), *nubbin/Pdm1*, Trypsin-like serine proteases β and ι, lysosomal α-mannosidases V and VI, *klumpfuss*, and members of the *E(spl)* gene complex *mα*, *mβ* and *m3* (Fig S1B-I). The scRNAseq data allowed us to order the cells in a pseudo-time axis (Street et al., 2018) along the transcriptional trajectories from the ISC/EBs cluster to the posterior midgut ECs (pECs) or the EE clusters (Fig 1H). This analysis showed that *emc* expression increases towards the pEC fate but decreases along the trajectory leading to the EE fate (Fig 1I). The enriched expression of *emc* in the absorptive lineage together with the known role of bHLH proteins in intestinal homeostasis suggested a function of *emc* in promoting EC differentiation.

Emc is required for ISC and EB differentiation

To examine a possible role for Emc in absorptive lineage differentiation, we used the MARCM method (Fig 2A-B; Lee and Luo, 1999) to generate mosaics of *emc* mutant clones in the posterior intestine (Fig 2C-G). Clones of the null allele emc^{AP6} (Fig S2A; Ellis, 1994) had fewer differentiated cells and were enriched in Dl-positive ISCs (Fig 2C-D, H and Table S1; Ohlstein and Spradling, 2007). Clones for the strong hypomorphic allele emc^{1} and the predicted transcriptional null $emc^{LL02590}$ showed similar enrichment in Dl-positive ISCs with respect to wild-type clones (Fig 2F-H). We

then knocked down *emc* in ISCs and EBs by RNA interference (RNAi) and traced their lineage using the *escargot* (*esg*) flip-out (FO) approach ("*esg*^{TS}*-FO*", see Fig 3A; Jiang et al., 2009). Knockdown of *emc* repressed the differentiation of ISCs and EBs, with the *esg*$^{+}$ cell nests, typically comprising 1-3 cells, often expanding into larger clusters (Fig 3C; Ohlstein and Spradling, 2006; de Navascués et al., 2012). This resembled the phenotype of a loss of Notch signalling in ISCs/EBs (Micchelli and Perrimon, 2006; Ohlstein and Spradling, 2007; 2006). However, these larger clusters did not display the level of unchecked growth and invasive behaviour observed when Notch signalling is repressed in this tissue (Micchelli and Perrimon, 2006; Patel et al., 2015); see also Fig 5A). Moreover, knockdown of *emc* in the ISC/EB compartment led to the loss of many *esg*$^{+}$ cell nests (identified by their expression of Hdc, an RNA binding protein expressed in ISCs and EBs in the same pattern as *esg*, see Fig S2B and (Resende et al., 2017) (Fig S2C, compare with the control in Fig 3B). This was due to apoptosis since co-expression of the effector caspase inhibitor p35 and *emc*-specific RNAi prevents the loss of *esg*$^{+}$ cells (Fig S2D). We conclude that *emc* is necessary for the differentiation and survival of ISCs and EBs.

emc maintains the commitment of EBs

Our findings that Emc is enriched in the absorptive lineage (EBs and ECs), and that its loss blocks EC differentiation, prompted us to investigate whether the loss of Emc in EBs could reverse commitment to the absorptive identity. To this end, we knocked down *emc* with RNAi in adult EBs using the conditional, EB-specific driver *NRE-Gal4, UAS-GFP*, *tub-Gal80*^{TS} (Zeng et al., 2010), and analysed the expression of the ISC marker Dl in the GFP-labelled cells. Indeed, *emc* knockdown caused EBs to re-acquire Dl expression, often while displaying reduced GFP signal (Fig 4A-B). This suggested that *emc*-depleted EBs were reverting their identity. To verify this, we used a flip-out lineage tracing approach to irreversibly label EBs ("*NRE*^{TS}*-FO*"; Fig 4C) and stained for the mitotic marker phospho-Histone H3S10. In contrast with unmodified EBs, which are post-mitotic and only produce ECs (Micchelli and Perrimon, 2006; Ohlstein and Spradling, 2006; Zeng and Hou, 2015), *emc*-depleted EBs can undergo cell division and generate Delta-positive proliferative cells (Fig 4D-E). This suggests that *emc*-deficient EBs can not only activate Dl expression but also de-differentiate into functional ISCs, capable of cell division.

emc acts in parallel with Notch to direct EC differentiation

Our loss of function analyses show that Emc is required for differentiation into the absorptive (EC) cell fate. We next assessed the capacity of *emc* to impose EC differentiation by overexpressing it with *esg*^{TS}*-FO*. Indeed, forced expression of *UAS-emc* resulted in all ISCs and EBs differentiating into ECs (Fig 5A), as previously reported (Lan et al., 2018). This establishes that Emc is both necessary and sufficient to direct differentiation towards the absorptive fate.

This phenotype is similar to that of over-activating the Notch pathway, a known regulator of ISC fate in both flies and mammals (Bardin et al., 2010; Micchelli and Perrimon, 2006; Ohlstein and Spradling, 2006, Fre et al., 2005; van Es et al., 2005) and suggests that *emc* might function through Notch signalling. To explore this possibility, we tested whether *emc* could force EC differentiation in the absence of Notch. Knockdown of *Notch* with *esg*^{TS}*-FO* leads to an invasive expansion of Dl-positive ISC-like and Pros-positive EE-like cells (Micchelli and Perrimon, 2006; Patel et al., 2015); see Fig 5B). When we co-expressed *emc* and *N*^{RNAi} together, all ISCs and EBs turned into ECs (Fig 5B), strongly suggesting that *emc* operates downstream of Notch. This phenotype, however, could also be due to the excess of Emc quickly driving cells irreversibly into differentiation before the knockdown of *Notch* resulted in effective clearance of Notch protein. To reduce Notch signalling with the same kinetics as the *UAS-emc* transgene transcription and translation, rather than the additive kinetics of *UAS-Notch*^{RNAi} transcription, RNAi biogenesis, RNA interference, and extant Notch protein decay, we overexpressed Hairless (H), the co-repressor associated to the nuclear effector of N^{ICD}, Su(H) (reviewed in Bray and Furriols, 2001), with *esg*^{TS}*-FO*. As expected, this leads to expansion of Dl-positive and Pros-positive cells, with a strong reduction of EC differentiation (Fig 5D-E; Bardin et al., 2010). By contrast, co-expression of *emc* and *H* led to a sharp increase in the levels of EC differentiation (Fig 5D, F). This further indicates that Emc can induce differentiation in the absence of Notch signalling.

Next, we tested whether *emc* mediates the effects of Notch signalling. Activating the pathway by knocking-down *H* leads to an increase in EC differentiation (Fig 5G; Bardin et al., 2010) and to the expression of the NRE reporter in all the progenitor, diploid cells, including those expressing Dl (Fig 5G); this is likely due to an increased baseline expression of the NRE reporter, as expected in the absence of H (Furriols and Bray, 2001). Simultaneously knocking down *H* and *emc* did enhance the increase in EC differentiation induced by knockdown of *H* (Fig 5D, H). Taken together, our data

suggest that Notch signalling is not epistatic over *emc* and therefore Emc may induce EC differentiation independently.

Emc antagonises self-renewal by disrupting Daughterless homodimers

A fundamental molecular function of Emc/Id transcriptional regulators consists in titrating class I and II bHLH transcriptional activators (Campuzano, 2001; Engel and Murre, 2001; Hasskarl and Munger, 2014; Norton, 2000; L.-H. Wang and Baker, 2015). Archetypal targets of this inactivation in *Drosophila* are Da and Sc, to which Emc binds directly *in vitro* and *in vivo* (Alifragis et al., 1997; Cabrera et al., 1994; Giot et al., 2003; Shokri et al., 2019; Van Doren et al., 1991). Therefore, the intestinal phenotypes we observed with the loss of *emc* may be due to increased activity of Da and its dimerization partners. Indeed, overexpression of *da* with esg^{TS}*-FO* strongly resembled the effect of *emc* knockdown. Differentiation was almost completely impaired (Fig 6A-B, I), while many *esg*-positive cell nests (labelled by *hdc* expression) were lost (Fig 6B), with their survival rescued by co-expression of p35 (Fig S3A). Conversely, loss of *da* promoted EC differentiation (Fig S3B-C and 6I), as previously described (Bardin et al., 2010; Lan et al., 2018) and mimicked the effects of Emc overexpression (Fig 5A). This suggests that the role of Emc is largely to repress one or more Da-containing bHLH dimers, which in turn maintain stemness and survival. Epistasis experiments further confirmed this: the simultaneous loss of Emc and Da led to the differentiation of ISCs and EBs into ECs (Fig 6E-H).

We sought to determine the identity of the Da partners involved in maintaining stemness. Most *Drosophila* class II bHLH factors (Moore et al., 2000) are expressed in the intestinal cell types ISC, EB, EC and EE at very low levels (Fig S3D); several of them are already known not to have an essential role in ISC maintenance (Bardin et al., 2010; Beebe et al., 2015; Hartenstein et al., 2017). However, Da can form homodimers (Cabrera et al., 1994; Cabrera and Alonso, 1991) in several contexts, and is often functionally antagonized by Emc (Andrade-Zapata and Baonza, 2014; Bhattacharya and Baker, 2011; D'Rozario et al., 2016; Tanaka-Matakatsu et al., 2014; Tapanes-Castillo and Baylies, 2004; Troost et al., 2015). To test whether Da:Da dimers were involved in preventing differentiation, we overexpressed forced Da homodimers using the *UAS-da:da* tethered construct (Neuhold and Wold, 1993; Tanaka-Matakatsu et al., 2014) with esg^{TS}*-FO*. This blocked the differentiation of ISCs and EBs, which accumulated in larger clusters (Fig 6C-D; Table S2). Expression of Da:Da did not lead to esg^{+} cell death (Fig 6D, compare nest density with 6B). This shows that Da homodimers prevent differentiation, but does not rule out that other Da-containing

complexes could also be necessary to maintain self-renewal. To test this, we took advantage of the *UAS-da*^{RNAi} transgene *P{TRiP.JF02488}*. *UAS-da*$^{RNAi\text{-}JF02488}$ targets the 5'UTR of the endogenous *da* transcript, which is absent in the *UAS-da:da* construct (Fig S3E), and it induced complete differentiation of the progenitor cells (Fig S3B and 6I). Thus, we co-expressed *da:da* and *da*^{JF02488} in ISCs and EBs to evaluate the capacity of Da:Da to prevent differentiation when the endogenous, monomeric Da cannot. The effects were identical to the overexpression of *UAS-da:da* alone (Fig S3F, compare with Fig 6D). This indicates that Da can promote ISC self-renewal solely as a homodimer, which is antagonised by Emc to allow EC differentiation. Furthermore, since both the overexpression of monomeric Da and the knockdown of *emc* (to raise levels of bHLH-containing complexes) induce *esg*$^{+}$ cell death (Fig 6B, S3A and S2CD), but the overexpression of Da:Da does not, it follows that the balance between Da and Emc contributes to *esg*$^{+}$ cell survival.

Basal levels of Sc in esg^{+} cells confer ISC properties

Our results show that the maintenance of self-renewal depends on Da homodimers. However, the loss of function phenotype of *emc* best mimics the effects of overexpressing monomeric Da, which is expected to increase the levels of any Da-containing complex where Da is limiting. Therefore, since depleting *emc* increased the levels of the ISC marker Dl, we reasoned that this increase might depend on another Da partner expressed in ISCs, such as Scute. Recent studies have shown that Sc is detectable in ISCs (Chen et al., 2018; Doupé et al., 2018), and members of the *AS-C* are proposed to promote Dl expression during neurogenesis (Hinz et al., 1994; Kunisch et al., 1994). Therefore, we tested whether the increased levels of Dl observed upon *emc* loss (Fig 3C-D) could be caused by elevated activity of Sc or any of the other bHLH factors belonging to the *AS-C*. We induced *emc* knockdown in MARCM clones, which were either wild-type or homozygous for *Df(1)sc*^{B57} (a deletion of the entire *AS-C*; González et al., 1989) and compared their respective levels of Dl expression using the signal from anti-Pros as normalisation factor (see Apendix). With this approach, we observed an average four-fold decrease in Dl levels in *emc*-depleted clones when they were homozygous for *sc*^{B57}, indicating that Sc and possibly other members of the *AS-C* are necessary to boost Dl expression in ISCs lacking Emc (Fig 7A-C).

These observations prompted us to ask whether Sc could contribute to the maintenance of stem cell characteristics in ISCs. Overexpression of Sc with *esg^{TS}-FO* clearly leads to increased differentiation into Pros-positive EEs (Fig 7D, H; Bardin et al., 2010; Chen et al., 2018). To evaluate whether Sc induces stem cell properties in EBs, similar to Emc knockdown, we overexpressed Sc with the EB-specific driver *NRE^{TS}-FO*. In contrast to wild-type EBs, which are post-mitotic, Sc-expressing EBs were capable of division, and their offspring included both Pros- and Dl-expressing cells, indicating the acquisition of ISC-like properties (Fig 7I, compare with Fig 4D). We conclude that Sc can induce stem-cell like characteristics in EB progenitors.

Sc:Da and Da:Da antagonise each other in the ISC-to-EE transition

We have so far provided evidence that Da homodimers maintain ISC self-renewal, and that Emc-mediated titration of Da triggers EC differentiation. EE differentiation, however, requires the transition from the transcriptional program of Da:Da to that of Da:Sc. Two main scenarios are possible: Sc:Da dimers could initiate a program that silences, or is epistatic to, that maintained by Da:Da dimers (“succession”). Alternatively, the relative strengths of the two programs could determine the fate outcome for the cell (“antagonism”). To distinguish between these alternatives, we evaluated the ability of an excess of Da monomer to suppress EE differentiation induced by overexpression of Sc with *esg^{TS}-FO*. Overexpression of *sc* in ISCs and EBs leads to a quick expansion of Pros-positive cells (Fig 7D; Bardin et al., 2010; Chen et al., 2018). These were often mitotic (Fig S4A, D), and the number of GFP^{+} cells generated in only 3 days of lineage tracing was much higher than those generated during normal tissue replacement (Fig 7D, compare with Fig 3B and Fig 6A). This phenotype depended upon the presence of Daughterless: the overexpression of Sc in *da*-depleted cells did not result in induction of Pros-positive cells (Fig S4E-G).This suggests that some of these cells have been trapped into a pre-EE state, where cells express both Pros and Dl and are also capable of mitosis (Chen et al., 2018; Zeng and Hou, 2015). However, the co-expression of Da with Sc greatly reduced the number of extra Pros-positive, Dl-negative cells and led to an increase in Dl-positive cells (Fig 7E, H), while maintaining mitotic figures (Fig S4B, D). Under these conditions, the amount of Sc:Da dimers is expected to be either similar or higher than with the overexpression of Sc alone (as endogenous *da* is expressed weakly, likely in limiting amounts; Bardin et al., 2010), but with a simultaneous increase in Da homodimers. In this case, the reduction of EE differentiation and increase of ISC population seen with Sc and Da overexpression would be indicative of antagonism between their respective

transcriptional programs, rather than their succession. If this is the case, we would expect that the co-expression of tethered Da:Da and Sc would result in even less EE differentiation, because the *UAS-da:da* transgene cannot contribute Da monomers to bind to Sc. Indeed this was what we observed experimentally: co-expression of Da:Da and Sc resulted in an even higher fraction of Dl-positive cells, at the expense of Pros-positive cell formation (Fig 7F, H), and with a concomitant increase in mitotic figures (Fig S4C, D).

To further test the capacity of Da homodimers to antagonise EE differentiation, we co-expressed *da:da* and *Notch*^{RNAi} with *esg*^{TS}*-FO*. On its own, the reduction of Notch leads to the formation of abundant Pros-positive EE-like cells (Bardin et al., 2010; Ohlstein and Spradling, 2006). However, Da:Da opposed the formation of extra Pros-positive cells under conditions of *Notch* loss (Fig 7G, compare with Fig 5B). This further indicates that Da:Da can oppose EE differentiation, and is consistent with a mechanism in which Sc:Da dimers need to overcome the activity of Da:Da dimers to induce the EE fate.

Da:Da and Da:Sc collaborate to promote ISC identity

Our data indicate that Da:Da and Sc:Da activate distinct and antagonistic transcriptional programs that maintain ISC self-renewal and initiate EE differentiation, respectively. However, during the development of the peripheral nervous system, both Da homodimers and Sc:Da heterodimers can direct the same cell specification (sensory organ precursor identity; Troost et al., 2015).

To determine the transcriptional signature induced by these factors, we performed RNA-seq analysis of purified *esg-Gal4 UAS-GFP* ISCs and EBs that overexpressed either *da*^{RNAi}, Da, Da:Da or Sc. Each experimental condition gave a distinct mRNA transcriptome signature (Fig 8A, Fig S5A and Table S3), with Sc overexpression inducing more widespread changes in gene expression. Overexpression of Da and Da:Da produced very similar effects, especially with respect to upregulated genes (all genes upregulated by Da:Da were also upregulated by Da). By contrast, the gene sets downregulated respectively by Da:Da and Da overexpression overlapped partially, with a sub-set of genes unique for Da:Da. Interestingly, the transcriptional effects of *da* depletion had substantial overlap with those of Da overexpression (Fig 8A). Using a panel of 57 cell type-exclusive marker genes for ISCs, EBs, pECs and EEs (Table S4 and Fig S5B), we found that both *da* knockdown and Da overexpression caused ISCs and EBs to reduce expression of EE-specific genes like the transcription factors *pros*

and *dimmed (dimm)*, the peptide hormones *AstA*, *AstB/Mip*, *AstC* and *Dh31,* and the secretory fate-promoting factor *phyl* (Yin and Xi, 2018) (Fig 8B and S5C). This likely reflects on one hand, the capacity of Da overexpression to generate excess Da:Da dimers that prevent EE differentiation (Fig 6C-D and Fig 7G), and on the other, the requirement for Da:Sc to induce EE genes (Y. Li et al., 2017); see also figure S4E-G). Consistent with this view, overexpression of Sc induced many EE-specific genes, but also the ISC-specific genes *spdo* and *Dl*. Overexpression of Da:Da or Da alone also induced some ISC-specific genes, for instance *mira* and (for Da:Da only) *spdo*. Inspection of the entire panel also revealed that EC- and EB-specific genes (*myo31DF*, *nub/pdm1*, α*Try*, β*Try*; *E(spl)m*β*-HLH*, *E(spl)m3-HLH*) tended to be upregulated by *da* knockdown and downregulated in the other three conditions, in agreement with our phenotypic observations (Fig S5B).

To determine whether the differentially regulated genes in these conditions might be direct targets of these bHLH factors, we analysed whether these genes had nearby regulatory elements containing E-boxes (the canonical binding sites of bHLH factors). Indeed, using the iCisTarget search tool (Herrmann et al., 2012), we found that E-boxes and other binding sites for class I and II bHLH factors were overrepresented in predicted regulatory elements close to genes that were upregulated by overexpression of Da or Da:Da, or downregulated by *da* depletion (Table 1, Fig 8C and Supplementary Table S5). Overexpression of Da and Da:Da led to the downregulation of genes that contained N-boxes (the binding target of E(spl) proteins of the bHLH family), possibly reflecting interference with Notch signalling effectors. Intriguingly, Sc overexpression resulted in the downregulation, rather than the upregulation, of genes enriched in bHLH-binding E-boxes (Fig 8C). Furthermore, the knock-down of *da* led to the upregulation of genes with a marked enrichment in GATA-boxes, likely due to the described role of *GATAe* in ISC differentiation (Okumura et al., 2016).

To characterise the molecular signature induced by Da:Da, Da, Sc and *da* knock-down more systematically, we used Gene Set Enrichment Analysis (GSEA; Subramanian et al., 2005) against previously described transcriptional profiles of midgut cell types (Dutta et al., 2015). The most obvious patterns were with da^{RNAi}, which clearly induced genes expressed in the absorptive lineage while reducing the expression of ISC- and EE-specific genes, and Sc overexpression, which did the opposite (Fig 8D). Sc also induced ISC-specific genes, and did so better than Da:Da in our experimental conditions. This seemed inconsistent with the observed capacity of Da:Da to prevent differentiation, and the described role of Sc in forcing terminal EE differentiation (albeit

at long time scales; Chen et al., 2018). Therefore, we looked at the expression changes in individual genes within the ISC-specific gene set. While both Da:Da and Sc induced regulatory genes such as *Dl* or *mira*, they had opposite effects on factors involved in DNA replication (*Orc2*, *Mcm2*, *Mcm5*, *Mcm6* and *Mcm7*) or in mitosis (*polo*, *aurB*, *BubR1* and *Ncd80*), which were repressed by Da:Da but induced by Sc. This is in agreement with the described roles of Sc as a mitotic inducer in the intestine (Chen et al., 2018) and of Da:Da as a repressor of cell cycle progression in imaginal discs (Andrade-Zapata and Baonza, 2014), but also highlights the capacity of Sc to regulate key ISC-specific genes, such as *Dl*. This feature was also confirmed in our analysis of adult midgut scRNAseq datasets described above, where cells classified as ISC/EBs that expressed *scute* had on average much higher levels of *Delta* (Fig S5D).

We wanted to determine whether manipulating *da* and *sc* in our experimental conditions had induced changes in specific cellular processes. Using the Gene List Annotation for Drosophila (GLAD) resource (Hu et al., 2015), we found that Da:Da, Da and Sc overexpression caused enrichment in categories involved in regulatory mechanisms (receptors, kinases, GCPRs or signalling pathways, with Notch singled out; Fig 8E). Interestingly, these treatments also down-regulated genes involved in mitochondrial function, oxidative phosphorylation and ribosomes, all gene sets enriched when *da* was knocked-down. Da:Da also downregulated metabolism genes (Fig 8E). Hence, we used the gene sets from the Kyoto Encyclopedia of Genes and Genomes (KEGG, (Kanehisa et al., 2023) to determine whether specific biochemical pathways were affected. We found that Da:Da negatively regulated genes involved in the metabolism of some lipids, glycosyl groups and amino acids (Fig 8F). This contrasted with the effect of da^{RNAi}, which increased expression of metabolic genes in several of these pathways (Fig 8E-F).

These results show that Da and Sc induce distinct signatures which actively promote the ISC and EE identities, respectively, but they also repress the active metabolism typical of EC function. Moreover, a sensitive balance of Da and Sc is required to maintain the transcriptional identity of the ISC and its proliferative capacity.

Da:Da is antagonised by Notch and maintains self-renewal in parallel to Esg

Esg, a Zinc finger factor of the Snail family, is a conserved regulator of ISC fate in both mice and flies. In *Drosophila* it is required to prevent ISC/EB differentiation, mostly through transcriptionally repressing differentiation genes (Horvay et al., 2015; Korzelius et al., 2014; Loza-Coll et al., 2014). Da:Da seems to have a similar effect, through the

activation of ISC-identity genes. Therefore, we sought to test whether Esg and Da might act in combination to maintain stemness. Knockdown of *esg* in ISCs and EBs led to differentiation, with an overrepresentation of EEs (Fig S6C and 9F), as expected from the described antagonism between Esg and Sc at the *pros* locus (Y. Li et al., 2017). Simultaneous overexpression of *UAS-esg*^{RNAi} and *UAS-da:da* prevented most differentiation, and specifically reduced EE cell production (Fig 9D, F), indicating that Da:Da can maintain ISCs and oppose EE differentiation independently of *esg*. In turn, overexpression of *esg* blocked differentiation irrespective of the presence of *da* (Fig 9C, F and Fig S6B), indicating that Da:Da and Esg largely act independently in ISC maintenance. Furthermore, expression of *da* was not affected by Esg levels and vice versa (Fig S6D, E), showing that *da* and *esg* are regulated independently of each other.

We next sought to determine whether Da:Da operates as part of a pathway with the known regulators of ISC fate. Our previous epistasis analysis with *emc* and Notch signalling components suggested that Da:Da is required independently of the Notch pathway. Indeed, when we depleted both *N* and *da* using RNAi with the *esg*^{TS}*-FO* driver, all ISCs/EBs differentiated into ECs (Fig S6A). Similar results were obtained by simultaneously depleting *da* and inhibiting Notch signalling by overexpressing *H* (Fig 9A, E, compare with Fig 5E). However, expressing *UAS-da:da* prevented the differentiation induced by increasing Notch signalling through knockdown of *H* (Fig 9B, E, compare with Fig 5G), suggesting that Da:Da can antagonise Notch signalling. Together, our data indicate that Da homodimers operate in parallel to Esg and downstream of Notch to maintain ISC self-renewal.

DISCUSSION

Multipotent adult stem cells must be able to switch their transcriptional state from self-renewal to distinct differentiation programs. bHLH transcription factors seem well placed to act as cell-intrinsic molecular switches; they have been described to operate synergistically, antagonistically or combinatorially (Amoutzias et al., 2008; Bhattacharya and Baker, 2011; Sallee et al., 2017; Troost et al., 2015) and their capacity for dimerization allows reduction in molecular noise (Bundschuh et al., 2003). Here we show that a bHLH factor network controls three alternate fates in the adult *Drosophila* intestine. Class I homodimers (Da:Da) promote the progenitor state of ISCs/EBs. Progenitor cells will acquire the absorptive fate by titration of Da by the HLH factor Emc, or the secretory fate by expression of the class II bHLH Sc, which heterodimerises with Da to initiate EE differentiation. Moreover, Emc is required in EBs to maintain their committed state, while low levels of Sc seem to boost essential parts of the ISC transcriptional program. Our results demonstrate a central role of bHLH factors in the acquisition and maintenance of multiple cell fates in the fly intestine.

Three fates regulated by a dimerization network

Our data indicated that Da homodimers maintain ISCs and EBs in an undifferentiated state, but that these cells can easily be pushed towards either EC or EE differentiation when Da:Da dimers are converted to Da:Emc or Da:Sc dimers (Fig 10). Similar networks involving class I, II and V bHLH factors regulate the development of the *Drosophila* retina (Bhattacharya and Baker, 2011) and the fly's peripheral nervous system (PNS) (Cubas et al., 1991; Troost et al., 2015; Van Doren et al., 1991). However, in these cases only one new fate is accessed (neural), and Da:Da dimers seem to have more of an accessory role, unlike the central one that we describe here for the intestine. In the retina, Da:Da dampens the titration by Emc of the bHLH proneural factor Ato (Bhattacharya and Baker, 2011; K. Li and Baker, 2018). In the PNS, Da:Da cooperate with Da:Ac/Sc heterodimers to overcome Emc inhibition and induce neural fate, which both Da:Ac/Sc and Da:Da can induce (Troost et al., 2015). By contrast, in the adult midgut Da:Da and Da:Sc promote distinct fates (progenitor and secretory, respectively) while Emc titrates both dimers to allow EC differentiation, enabling the network to execute a three-way fate decision. This may be possible because Da:Da and Da:Sc induce specific but partially overlapping transcriptional profiles (Fig 8) which seem to be able to act antagonistically (Fig 7). By contrast, Emc simply prevents the DNA binding of either Da or Sc (Cabrera et al., 1994; Van Doren et

al., 1991), which suggests that EC is the default fate when Da:Da dimers are absent (Fig 6).

Interestingly, bHLH transcription factors of classes I, II, and V (or E/A/Id) are also active in the mammalian intestine. Class II bHLH factors promote EE differentiation (reviewed in Philpott and Winton, 2014) and ISC maintenance (van der Flier et al., 2009). However, the class I factors E2a and Heb are specifically expressed in crypt cells in the mouse intestine (van der Flier et al., 2009). Our work suggests that they might function as class I dimers as well as dimerization partners for class II factors. Meanwhile, Emc homologs Id2 and Id3 are expressed specifically in differentiated murine intestinal epithelial cells (Wice, 1998), suggesting a similar function in absorptive enterocyte differentiation. By contrast, Id1 is required in ISCs for regeneration (N. Zhang et al., 2014) and can act as an oncogene (Wice, 1998), which is the opposite behaviour to that of Emc.

A balance of bHLH factors regulates intestinal stem cell fate

Our observations indicate that additional work on the mechanisms that regulate the transcription of both *emc* and *sc* should be very informative. The *cis*-regulatory region of *emc* seems to be complex and spreads across a large genomic region (K. Li and Baker, 2019), so it is likely subject to multiple regulatory inputs. An obvious candidate for regulation of *emc* transcription is Notch signalling, as shown in other contexts (Adam and Montell, 2004; Baonza et al., 2000; Baonza and Freeman, 2001; Bhattacharya and Baker, 2009; Spratford and Kumar, 2015) and considering the importance of Notch for EB establishment and EC differentiation (Bardin et al., 2010; Micchelli and Perrimon, 2006; Ohlstein and Spradling, 2006). However, our epistasis analyses suggest that Emc and Notch signalling may induce EC differentiation independently of each other, an observation that makes Notch an unlikely regulator of *emc* in the midgut. A major regulator of Sc is the transcriptional repressor Ttk69 (C. Wang et al., 2015), whose stability is in turn regulated by the E3 ubiquitin ligase Sina and its adaptor Phyl (Yin and Xi, 2018). Therefore, Phyl expression could be the trigger to allow the accumulation of Sc and initiate EE differentiation. How *phyl* is regulated is not known yet. On the other hand, Chen et al. (2018) observed that Sc activates itself as well as *E(spl)m8*, a member of the *Enhancer of split Complex* (which comprises several transcription factors, many of which are often both targets and effectors of the Notch pathway; reviewed in Delidakis et al., 2014). As E(spl)m8 is able to repress Sc, the authors proposed that a cell-autonomous oscillator involving Sc and *E(spl)-C* members would create pulses of Sc expression which would set the pace of EE

production (Chen et al., 2018). However, while we too observe induction of *E(spl)-C* genes upon Sc overexpression, we also see this as a result of Da:Da and Da overexpression (Fig S5E). This suggests that the regulation of *E(spl)-C* (and therefore of *sc*) may be more complicated. Additional work will be necessary to determine the sequence and timing of regulatory inputs that initiate fate-inducing levels of Sc or Emc.

Moreover, the Emc/Da/Sc network clearly does not work as a simple Boolean switch. The three genes are expressed and functionally relevant in both ISCs and EBs (Bardin et al., 2010; Chen et al., 2018; Doupé et al., 2018); this work). This argues against a mechanism that simply initiates Emc or Sc expression to induce the EC or EE fates. Moreover, the functions of Emc and Sc seem to be more complex than acting as mere fate inducers. While Emc is critical for absorptive differentiation, in this lineage commitment and terminal differentiation are separated in time, with EBs being produced well before their terminal differentiation occurs (Antonello et al., 2015). This 'pause' after commitment requires adequate levels of Emc in the EB, as its depletion induces de-differentiation into ISCs (Fig 4), but its overexpression accelerates EB terminal differentiation into ECs (Fig 5). Intriguingly, it has been proposed that the Emc homolog Id1 protects pluripotency in the epiblast of the mouse embryo specifically during the peri-implantation transition (Malaguti et al., 2019). This suggests that Emc could be part of a mechanism that times the ISC→EB→EC transition, transiently protecting the committed and undifferentiated state of the EB. As for Sc, our data suggests that the low levels of Sc found in ISCs (Chen et al., 2018; Doupé et al., 2018) induce the expression of ISC-specific genes (Fig 8) without eliciting a conversion into pre-EE cells. Higher levels appear to be required to initiate EE differentiation. Therefore, the amounts of Da, Sc and Emc must be maintained in a delicate balance. In the case of Emc, this is possibly achieved through post-transcriptional mechanisms. During neurogenesis, Emc is stabilised when bound to Da, and degrades when Da frees itself to bind a proneural factor (Bhattacharya and Baker, 2011; K. Li and Baker, 2018). This may be the reason that Emc shows higher levels of accumulation in EBs and ECs (Fig 1), where Da is expressed but other bHLH factors are at minimal levels (Fig S3).

The fine tuning of the relative amounts of Da and Emc affect not only the fate of ISCs and EBs, but their survival too, as either Da overexpression or *emc* depletion leads to apoptosis (Fig 6B, S3A and S2CD). However, overexpressing tethered Da:Da dimers, which cannot be titrated by Emc, do not lead to cell death. It is therefore possible that Da forms complexes with a yet unidentified partner to promote cell death in *esg*$^{+}$ cells

through transcriptional regulation, and that these complexes are titrated by Emc. However, Emc can also bind non-HLH proteins in vitro (Hr78; Shokri et al., 2019) and in vivo (Abd-A, Ubx; Bischof et al., 2018); it is possible that there are Emc-containing complexes that promote survival and be titrated by Da monomers.

Da and Sc cooperate to endow cells with ISC properties

Our data show a critical requirement for Da:Da in ISC maintenance, but also that Sc can contribute to enhance ISC features (proliferation, expression of Dl). This is likely an active promotion of ISC fate, rather than just prevention of differentiation, as our transcriptomic analysis shows a significant enrichment of the ISC transcriptional signature when Sc is overexpressed (Fig 8D). The existence of this active role is further supported by the capacity of Sc to induce EBs to de-differentiate into ISCs and re- or transdifferentiate into EEs (Fig 7). We also find evidence that mitochondrial function is reduced by expression of Sc, Da and Da:Da, which fits well the observation that ISCs display an 'empty mitochondria' phenotype under the electron microscope (Hung et al., 2020). By contrast, knocking down *da* increases expression of nuclear genes involved in mitochondrial function (Fig 8); this would be consistent with the metabolic requirements of the EC fate. However, it has recently been shown that the EGFR pathway stimulates ISC proliferation by inducing mitochondrial biogenesis, β-oxidation and oxidative phosphorylation (C. Zhang et al., 2022). Therefore, the downregulation of mitochondrial genes by Da:Da, Da and Sc could reflect their function in maintaining the ISC fate against EC differentiation but, in the case of Da:Da it could also be part of a role promoting the quiescence of the ISC. This would be compatible with the effect of *da* as a repressor of cell cycle progression in imaginal disks (Andrade-Zapata and Baonza, 2014) and our observation that Da:Da represses mitotic genes (Fig S5). Together, this suggests that Da:Da dimers are essential to maintain the ISC in an undifferentiated state, but low levels of Sc:Da dimers also contribute to the maintenance of the ISC identity and function. We surmise that Emc expression in EBs would be required to dampen this Sc activity to prevent untimely EE differentiation and mitotic cell cycle activation in the EB.

Regulation of the committed state of the enteroblast

Under normal conditions, EBs will only give rise to mature ECs without further division (C. Wang et al., 2015; Yin and Xi, 2018; Zeng and Hou, 2015). Depletion of Emc specifically and heritably in EBs resulted in cells that expressed Dl as well as proliferation markers (Fig 4), which likely represents a de-differentiation process. This

may partially reflect the need to control Sc activity in the EB, as the expression of Sc induced similar effects (Fig 7). Intriguingly, depletion of Ttk69 or Klu in EBs or overexpression of Phyl seem to induce trans-differentiation, as these conditions produce Pros-positive cells (C. Wang et al., 2015; Yin and Xi, 2018); Korzelius et al., 2019; Reiff et al., 2019). This difference could be because Emc influences the activity of multiple Da-containing complexes in the EB, or because of the activity of additional targets of Klu and the Phyl/Ttk69 pathway apart from Sc. The reacquisition of proliferation and Delta expression is also controlled by other factors, such as Sox21a (Zhai et al., 2015), or the global co-repressor Gro, acting downstream of Notch (X. Guo et al., 2019) (though surprisingly Notch itself does not seem to be required to maintain the EB; Siudeja et al., 2015). Together with our observations, this indicates a previously unappreciated plasticity of the EB, which is consistent with its similarity to the ISC in transcriptome composition (Hung et al., 2020) and chromatin accessibility landscape (Aughey et al., 2018). Importantly, this resembles the behaviour of EC precursors in the mammalian intestine, which can dedifferentiate and repopulate the intestinal crypt during regeneration (Tetteh et al., 2016).

In summary, our study highlights the plasticity of absorptive committed precursors of the adult intestine and identifies key roles for conserved bHLH factors in the homeostatic maintenance this tissue, where the functional and protein-protein interactions between these factors form a three-way switch between two differentiation lineages and self-renewal.

MATERIALS AND METHODS

Drosophila culture and genetics

Flies were raised and maintained on standard cornmeal/yeast medium at 25ºC unless specifically indicated. Experiments were conducted in mated females, collected daily and maintained in fresh vials with added yeast until 4-7 days old. For experiments using Gal80^{TS}, flies were reared and aged to gut maturity (~7 days) at 18ºC, then transferred to 29 ºC. For induction of MARCM and flip-out clones, 4-7 days old flies were treated at 37ºC for 60 or 15 min, respectively. Flies were aged for 7 days after induction treatment before dissection, unless otherwise indicated. See Appendix for fly strains.

Immunohistofluorescence, confocal microscopy and image analysis

Stainings were performed as in Bardin et al., (2010). See Appendix for details on primary and secondary antibodies. DNA dye was Hoechst (Sigma-Aldrich B2261 used 1:5000 from a stock solution at 10 mg/ml). Mounting medium was 4% N-propyl-galate, 80% glycerol. Confocal stacks were obtained in a Zeiss LSM 710 with an EC Plan-Neofluar 40X oil immersion objective (numerical aperture 1.3). All stack positions were acquired in the posterior midgut. Typically, three positions along the anterior-posterior axis of the posterior midgut were acquired for each organ. In MARCM clone experiments, stacks were acquired from all clones in the posterior midgut. Figures were assembled using Adobe Photoshop and Illustrator CS6 and Affinity Designer 2.

Cell counts and statistics

For evaluating the proportion of cell types in GFP^{+} clones or labelled tissue, confocal stacks were maximum-intensity projected using FIJI/ImageJ (Schindelin et al., 2012), cells of the relevant types were counted with the Cell Counter plugin. In the experiments overexpressing *UAS-sc* and *UAS-da:da*, the associated increase in proliferation generated large, highly densely populated cell clusters which could not be counted with single-cell precision. Therefore, for this genotype we estimated the proportion of each cell population in each field of view separately. See the Appendix for details on cell type identification.

Statistical tests were performed in Prism 8 or in R (R Core Team, 2023) using RStudio 2023.3.0.386 (Posit Software PBC, 2022). Statistical significance of changes in

proportions of cell types was assessed by binomial logistic regression in base R. We used Firth's bias reduced logistic regression (package *logistf*; Heinze et al., 2023) in experiments with zero observations in one or more of the genotypes considered, to avoid the nonsensical results arising from the 'complete separation' of data (Albert and Anderson, 1984).

RNA-seq

Flies bearing either *UAS-da*, *UAS-da*^{RNAi} (TRiP.JF02092), *UAS-da:da* or *UAS-sc* as well as *esg-Gal4*, *UAS-GFP* and *tub-Gal80*^{TS} were reared at 18ºC until 4-7 days old, transferred to 29ºC for 2 days and their midguts dissected, then processed as described in Dutta et al., (2013). Libraries from three biological replicates per condition (except one condition, with two) were prepared in two batches and ~37 million reads (either 50 or 300bp long, for each batch respectively) were generated per library using Illumina technology (Genewiz GmbH, Leipzig, Germany). Sequencing files are deposited at the Gene Expression Omnibus with accession number GSE234019.

RNA-seq and scRNA-seq analysis

Fastq read files, with adaptors pre-trimmed by the sequencing provider, were mapped to the release 6.28 of the *Drosophila melanogaster* genome using *STAR* and *bamtools* (Barnett et al., 2011; Dobin et al., 2013) and assigned to genes with *featureCounts* (Liao et al., 2014). Differential gene expression, gene set and DNA motif enrichment analyses were performed with the key R packages *DEseq2* (Love et al., 2014), *limma* (Ritchie et al., 2015), *fgsea* (Korotkevich et al., 2021) and *RcisTarget* (Aibar et al., 2017). scRNAseq data were obtained from GEO and https://flycellatlas.org. To correct for variability arising from technical and biological effects, we used the *IntegrateData* function in *Seurat* (Stuart et al., 2019; Hao et al., 2021). The *Slingshot* library (Street et al., 2018) was used for the trajectory analysis, which focused on ISC/EB cells as the initial state, pEC and EE cells, resulting in the identification of two distinct trajectories. The analysis code is in GitHub (Puigetal2023_bioinformatics_scripts) and archived at Zenodo including all input and output data (doi: 10.5281/zenodo.8116966).

ACKNOWLEDGEMENTS

We thank Nicholas Baker, Allison Bardin, Antonio Baonza, Sonsoles Campuzano, Sangbin Park, Mike Taylor, Shinya Yamamoto, Alfonso Martínez-Arias, the Bloomington *Drosophila* Stock Center, the Vienna *Drosophila* Resource Center, the *Drosophila* Genetics Resource Center (Kyoto) and the National Institute of Genetics (Japan) for providing fly stocks, and the Developmental Studies Hybridoma Bank (University of Iowa) for supplying antibodies. We also thank Juan Modolell, Sonsoles Campuzano, Catherine Hogan, Fernando dos Anjos-Afonso, Florian Siebzehnrubl, Terrence Trinca, Sonia López de Quinto, Helen White-Cooper, Mike Taylor and Wynand van der Goers van Naters for critical comments on the manuscript and useful discussions. We acknowledge the data analysis team of the College of Biomedical and Life Sciences of Cardiff University and the FACS and Imaging Core Facility at the Max Planck Institute for Biology of Ageing for technical assistance.

This work was supported by funding from Cardiff University to JdN and AP, from the University of Essex and NC3Rs SKT grant NC/W001047/1 to PVW and JdN, a DFG-Grant KO5594/1-1 and an EMBO Long-Term Fellowship to JK, a FAPESP fellowship #2021/00393-9 to VDN, a FAPESP São Paulo Excellence Chair #2019/16113-5 to PVW, and an ERC Advanced Grant no. 268515 to BAE.

JdN dedicates this work to the memory of Juan Modolell and Rosa María Aguilar.

AUTHOR CONTRIBUTIONS

Conception of the study and supervision: JdN. Data acquisition: AP, SD, SA, JK and JdN. Analysis and interpretation: AP, VDN, JdN, JK. Training and supervision: JdN, JK, PVW, BE. Writing the manuscript: JdN, AP. Revising and approval of the manuscript: all authors.

CONFLICT OF INTEREST

The authors declare no competing interest.

FIGURE LEGENDS

Figure 1. *emc* is expressed preferentially in the absorptive lineage.
A-E. Projected confocal stacks (A-B, D-E) showing endogenous Emc:GFP expression, and schematic illustrating the ISC lineage and our usage of cell type markers (C): ISCs are recognised by Dl expression; EEs by Prospero; EBs by NRE-lacZ; ECs by *myoIA-lacZ* and being polyploid. Emc is expressed in EBs (marked with *NRE-lacZ*, arrowheads in A, A') and most ECs (positive for *myoIA-lacZ*, solid arrowheads in B, B') but not all (empty arrowhead in B, B'). *emc* expression can also be detected in some ISCs (Dl^+) and EEs ($Pros^+$) (solid arrowheads and asterisks, respectively, in C-D') but not all (empty arrowheads and asterisks in C-D'). **F, G.** Expression of *emc* (E) and the EC marker *myoIA* (F) by scRNAseq in EEs, ISCs, EBs and ECs from the posterior midgut (pECs). Both genes are enriched in EBs and ECs, with rare events of detection in EEs and ISCs. **H.** Pseudotime trajectories from ISC/EB cells into mature EEs or ECs derived from scRNAseq data. **I.** *emc* expression in single cells declines as these get closer to the EE fate and increases as they progress towards EC differentiation.

Figure 2. *emc* is necessary for differentiation.
A-B. MARCM method: the FRT-FLP system is used to induce mitotic recombination in G2, which during mitosis (M) can result in co-segregation of sister chromatid arms (A). (B) After clonal induction, a subset of ISCs generate sparse labelled clones that can be followed up as tissue turns over. **C-G.** Differentiation is impaired in *emc* mutant clones. Control clones display more polyploid Dl^-/$Pros^-$ ECs (asterisks in C, F) than clones homozygous of for the mutant alleles emc^{AP6} (D), emc^{1} (E) and $emc^{LL02590}$ (G), which are enriched in Dl^+ ISCs (solid arrowheads) and diploid Dl^-/$Pros^-$ EBs (empty arrowheads) with respect to controls. **H.** Stacked bars plots aggregating cell type composition of MARCM clones shown in C-G. Numbers (cells/clones): control *FRT80B*, 310/117; emc^{1}, 112/95, emc^{AP6}, 208/200; control *FRT2A*, 194/106; $emc^{LL02590}$, 213/118. *p*-values are <0.05, <0.01 and <0.001 for one, two or three asterisks (see Tables S1 and S2 for further details). **I.** Types of cells considered in this work, with their colour representation and the markers used for their classification throughout the paper. Scale bars: 20μm.

Figure 3. *emc* is required for differentiation into mature ECs.
A. Use of the esg^{TS}*-FO* system allows the simultaneous manipulation and tracing of ISCs and EBs. *esg-Gal4, UAS-GFP* is expressed specifically in ISCs/EBs after induction (left panel) and activates irreversibly in ISCs/EBs the ubiquitous

Actin5C-Gal4, which in turn will maintain *UAS-GFP* expression if differentiation or commitment occur (right panel). **B-D.** ISCs and EBs in *esg^{TS}-FO* control guts produce both EC (Dl^{-}/Pros^{-}) and EE (Dl^{-}/Pros^{+}) GFP^{+} cells (B, note the difference in intensity levels between Dl and Pros, solid and empty arrowheads, respectively); differentiation is reduced when ISCs/EBs express *emc*-specific RNAi, shown by increased number of Dl^{+}/GFP^{+} cells (C, D). Reduction of *emc* also induces increased Dl expression: compare Dl-expressing with Pros-expressing cells (respectively solid and empty arrowheads in C, D), with those similarly marked in B. **E.** Stacked bars plots aggregating the cell type composition of *esg^{TS}-FO* tissue from B-E. Numbers (total GFP^{+} cells / fields of view): control, 1046/15; *UAS-emc$^{RNAi}{}_{NIG}$,* 104/21; *UAS-emc$^{RNAi}{}_{KK+HMS}$,* 832/15. p-values are <0.05, <0.01 and <0.001 for one, two or three asterisks (see Tables S1 and S2). Scale bars: 20μm in all panels.

Figure 4. *emc* is required for maintenance of the EB committed state.
A-B. The *NRE-Gal4* driver is expressed in EBs at different levels in normal intestines (solid and empty arrowheads in A for higher and lower-expressing EBs), but never co-express Dl. When *emc* is depleted with *NRE-Gal4*, many EBs co-express Dl (empty arrowheads, B) but not all (solid arrowheads, B). Also, EEs develop close to *emc*-depleted EBs (arrow, B). **C.** Use of *NRE^{TS}-FO* allows the simultaneous manipulation and tracing of the EB lineage. *NRE-Gal4, UAS-GFP* is expressed specifically in EBs after induction and activates specifically in EBs the (potentially) ubiquitous *Actin5C-Gal4*, which in turn will maintain *UAS-GFP* expression if differentiation or decommitment occur. **D-E**. Loss of *emc* in EBs leads to their decommitment. Activation of *NRE^{TS}-FO* in control guts leads exclusively to the labelling of EBs and ECs, with no co-expression of GFP and Dl or Pros (solid and empty arrowheads, respectively, in D; some ISCs and EEs in the micrograph seem inside the GFP territory due to the Z-projection of the confocal stack). By contrast, in *NRE^{TS}-FO* guts where *emc* is depleted, EB-derived cells express Dl and are capable of mitosis, as judged by phospho-Histone H3S10 staining (arrowhead in E-E''). Scale bar: 20μm in all panels.

Figure 5. *emc* induces EC differentiation in parallel to Notch signalling.
A. Forced expression of *emc* in ISCs/EBs induces differentiation into ECs: 99.4% of GFP^{+} were ECs; ISCs, EBs and EEs were 0.2, 0.2 and 0.4%, respectively; data from 812 cells from 10 fields of view). **B.** EC differentiation is abolished with knockdown of *N*, where there is accumulation of Dl^{+} (solid arrowheads) or Pros^{+} (empty arrowheads) cells. **C.** Simultaneous knockdown of *N* with overexpression of *emc* induces EC

differentiation (arrowheads). **D.** Stacked bars plots aggregating the cell type composition of *esg*^{TS}*-FO* tissue from E-H. Numbers (total GFP$^+$ cells / fields of view): *UAS-H*, 1810/21; *UAS-H+UAS-emc*, 1292/27; *UAS-H*$^{RNAi}_{HMS}$, 984/15; *UAS-H*$^{RNAi}_{HMS}$*+UAS-emc*$^{RNAi}_{NIG}$, 126/16. p-values are <0.05, <0.01 and <0.001 for one, two or three asterisks (see Tables S1 and S2). **E-F**. Overexpression of *H* strongly impairs EC differentiation and leads to accumulation of Dl$^+$ (solid arrowheads) or Pros$^+$ (empty arrowheads) cells (E). Simultaneous overexpression *emc* induces EC differentiation (F), but to a lesser an extent than in the background of *N* knockdown (asterisks in F, compare with C). **G-H.** Depletion of *H* induces EC differentiation (G) even in the absence of *emc* (G, D). Scale bars: 20*µ*m.

Figure 6. Da homodimers prevent differentiation and are antagonised by Emc.
A-D. Da homodimers maintain ISCs/EBs undifferentiated. Solid arrowheads: ISCs/EBs; empty arrowheads: ECs/EEs. Overexpression of Da with *esg*^{TS}*-FO* prevents formation of ECs, though it allows EE differentiation (B, compare with A). Expression of a forced Da:Da dimer in esg$^+$ cells prevents all differentiation, as evaluated with Hdc/NRE-lacZ (C) or Dl (D). **E-H.** *da* is epistatic over *emc*. Solid arrowheads: ECs; empty arrowheads: Dl$^+$ ISCs. MARCM clones mutant for *da*^{10} differentiate as ECs (E). This phenotype is recapitulated when these clones simultaneously express *emc*-specific RNAi (F). Likewise, impaired differentiation in *emc*^{LL02590} clones (G) is rescued by simultaneous knockdown of *da*, which leads to EC formation (H). **I.** Stacked bars plots summarising the cell type composition of *esg*^{TS}*-FO* tissue. Numbers (total GFP$^+$ cells / fields of view) are 1135/15, 549/14, 693/13, 803/15 and 1086/19 for control, *UAS-da*, *UAS-da:da*, *UAS-da*$^{RNAi}_{JF}$ and *UAS-da*$^{RNAi}_{HMS}$, respectively. P-values are <0.05, <0.01 and <0.001 for one, two or three asterisks (see Tables S1 and S2). Scale bars: 20*µ*m.

Figure 7. Sc:Da and Da:Da antagonise each other in EE formation but collaborate in ISC maintenance.
A-C. Emc antagonises Sc in inducing Dl expression. Loss of the *AS-C* using the *sc*^{B57} deficiency reduces the increase in Dl expression observed with knockdown of *emc* (B, compare with A). Dl levels are quantified by comparison with those of Pros (see Appendix). Numbers (Dl$^+$ cells/Pros$^+$ cells) are 210/146 and 718/210 for *UAS-emc*$^{RNAi}_{NIG}$ and *UAS-emc*$^{RNAi}_{NIG}$, *Df(1)sc*^{B57}, respectively. P-values are <0.05, <0.01 and <0.001 for one, two or three asterisks (Mann-Whitney test). **D-F.** Antagonism/collaboration between Sc and Da. Solid arrowheads: Dl$^+$/Pros$^+$ pre-EEs; empty arrowheads: Dl$^+$ ISCs; asterisks: Pros$^+$ EEs. Overexpression of Sc leads to a dramatic increase of Dl$^+$/Pros$^+$ pre-EEs and Pros$^+$ EEs, but maintains a population of

Dl$^+$ ISCs (D). The population of ISCs progressively increases by co-expression of monomeric Da (E) and dimeric Da:Da (F), at the cost of EE differentiation (E, F) and pre-EE formation (F). Quantified in H. **G.** Da:Da antagonises EE formation. While reduction of Notch signalling leads to an excess of EEs, simultaneous overexpression of Da:Da and *N*-specific RNAi results in very few Pros$^+$ cells (solid arrowheads, compare with Fig 5A). **H.** Stacked bars plots summarising the cell type composition of *esg^{TS}-FO* tissue. Numbers (total GFP$^+$ cells / fields of view) are 1241/6, 2131/10 and not determined/11 for *UAS-sc, UAS-sc, UAS-da*, and *UAS-sc, UAS-da:da*, respectively. p-values are <0.05, <0.01 and <0.001 for one, two or three asterisks (see Tables S1 and S2). **I.** Sc can induce decommitment of EBs. Expression of Sc with *NRE^{TS}-FO* leads to reacquisition of ISC properties (Dl expression, mitosis assessed with phospho-Histone H3S10, empty arrowhead) and pre-EE formation (Pros expression and mitosis, solid arrowhead). Scale bars: 20μm.

Figure 8. Da and Sc cooperate to induce expression of the ISC signature.
A. Euler diagrams showing the intersections of sets of genes either upregulated (left) or downregulated (right) by *da^{RNAi}*, Da:Da, Da and Sc, with $\log_2$ fold changes > 1.5 and adjusted p-values < 0.05. The area of the sets denotes (approximately) the size of the intersection. **B.** MA plots for the overexpression of *da^{RNAi}*, Da:Da, Da and Sc, respectively. Some genes of interest are identified because of their role or expression pattern. Colours match the cell types where genes are expressed. **C**. Beeswarm plots of the normalised enrichment scores of DNA motifs found in upregulated at $\log_2$FC ≥ 1.5 (brown, left) or downregulated at $\log_2$FC ≤ 1.5 (blue, right) genes in the four conditions analysed, using RcisTarget. Dots represent individual motifs, binned for simplicity of representation, and coloured by the type of transcription factor they are bound by. Those specifically bound by Da, Sc and E(spl) proteins are identified. **D-F**. Heatmaps of gene set enrichment scores for sets of genes that are: expressed in specific cell types (Dutta *et al*, 2015) (D), annotated because of their broad molecular function in *Drosophila* (Hu *et al*, 2015) (E) or belonging to annotated KEGG pathways (F). Asterisks indicate the enrichment scores with significant adjusted p-values, with colour indicating the level of significance. The colourmap of NES scores corresponds to different values in each heatmap.

Figure 9. *da* is epistatic to Notch signalling but acts in parallel with *esg*.
Solid arrowheads: ISCs (Hdc$^+$/NRE$^-$ or Dl$^+$/NRE$^-$); empty arrowheads: EEs (Pros$^+$). **A-B.** *da* is epistatic over Notch signalling. Loss of *da* leads to EC and EE differentiation when Notch signalling is impaired by overexpression of *H* (A), while overexpression of

da:da maintains cell undifferentiated even when Notch signalling is exacerbated by knockdown of *H* (B). **C-D.** *da* and *esg* function in parallel to prevent differentiation. Overexpression of *esg* can prevent differentiation and compensate for the loss of *da* (C), while overexpression of *da:da* can similarly compensate for the loss of *esg*, including prevention of EE formation (D). **E-F.** Stacked bars plots summarising the cell type composition of esg^{TS}-*FO* tissue. Numbers (total GFP^+ cells / fields of view) are 1510/21, 1810/21, 613/8 and 984/15 for *UAS-H*, *UAS-H+UAS-*$da^{RNAi}{}_{JF}$, *UAS-*$H^{RNAi}{}_{HMS}$ and *UAS-*$H^{RNAi}{}_{HMS}$*+UAS-da:da*, respectively (E) and 850/9, 1236/12, 628/18 and 939/19 for for *UAS-esg UAS-esg+UAS-*$da^{RNAi}{}_{JF}$, *UAS-*$esg^{RNAi}{}_{HMS}$ and *UAS-*$esg^{RNAi}{}_{HMS}$*+UAS-da:da*, respectively (F). p-values are <0.05, <0.01 and <0.001 for one, two or three asterisks (see Tables S1 and S2 for further details). Scale bars: 20μm.

Figure 10. Model of regulation of self-renewal and differentiation in the intestine by Sc, Da and Emc.

Orange arrows: Da homodimers maintain ISCs and EBs undifferentiated, antagonising EC differentiation and pre-EE formation by inducing expression of ISC-specific genes. Pink arrows: An increase of Sc expression induces formation of Da:Sc heterodimers, which steer the transcriptional program towards pre-EE formation; Sc can also induce expression of the ISC-specific signature, potentially leading to EB decommitment if its activity is not prevented by titration by Emc. Green arrows: Emc increased expression in EBs maintains commitment for EC differentiation and can direct terminal EC differentiation by interruption of Da:Da and Da:Sc transcriptional activities. This occurs in parallel to Esg prevention of differentiation and Notch signalling being upstream and opposing Da:Da to induce EC differentiation.

REFERENCES

Adam, J.C., Montell, D.J., 2004. A role for extra macrochaetae downstream of Notch in follicle cell differentiation. Development 131, 5971–5980. doi:10.1242/dev.01442

Aibar, S., González-Blas, C.B., Moerman, T., Huynh-Thu, V.A., Imrichova, H., Hulselmans, G., Rambow, F., Marine, J.-C., Geurts, P., Aerts, J., van den Oord, J., Atak, Z.K., Wouters, J., Aerts, S., 2017. SCENIC: single-cell regulatory network inference and clustering. Nat Methods 14, 1083–1086. doi:10.1038/nmeth.4463

Albert, A., Anderson, J.A., 1984. On the existence of maximum likelihood estimates in logistic regression models. Biometrika 71, 1–10. doi:10.1093/biomet/71.1.1

Alifragis, P., Poortinga, G., Parkhurst, S.M., Delidakis, C., 1997. A network of interacting transcriptional regulators involved in Drosophila neural fate specification revealed by the yeast two-hybrid system. Proc Natl Acad Sci USA 94, 13099–13104.

Amcheslavsky, A., Song, W., Li, Q., Nie, Y., Bragatto, I., Ferrandon, D., Perrimon, N., Ip, Y.T., 2014. Enteroendocrine Cells Support Intestinal Stem-Cell- Mediated Homeostasis in Drosophila. CellReports 1–19. doi:10.1016/j.celrep.2014.08.052

Amoutzias, G.D., Robertson, D.L., Van de Peer, Y., Oliver, S.G., 2008. Choose your partners: dimerization in eukaryotic transcription factors. Trends Biochem. Sci. 33, 220–229. doi:10.1016/j.tibs.2008.02.002

Andrade-Zapata, I., Baonza, A., 2014. The bHLH Factors Extramacrochaetae and Daughterless Control Cell Cycle in Drosophila Imaginal Discs through the Transcriptional Regulation of the cdc25 Phosphatase string. PLoS Genet 10, e1004233–16. doi:10.1371/journal.pgen.1004233

Antonello, Z.A., Reiff, T., Ballesta-Illan, E., Dominguez, M., 2015. Robust intestinal homeostasis relies on cellular plasticity in enteroblasts mediated by miR-8-Escargot switch. EMBO J. doi:10.15252/embj.201591517

Aughey, G.N., Estacio Gomez, A., Thomson, J., Yin, H., Southall, T.D., 2018. CATaDa reveals global remodelling of chromatin accessibility during stem cell differentiation in vivo. eLife 7, 6061. doi:10.7554/eLife.32341

Baonza, A., de Celis, J.F., Garcia-Bellido, A., 2000. Relationships between extramacrochaetae and Notch signalling in Drosophila wing development. Development 127, 2383–2393.

Baonza, A., Freeman, M., 2001. Notch signalling and the initiation of neural development in the Drosophila eye. Development 128, 3889–3898.

Bardin, A.J., Perdigoto, C.N., Southall, T.D., Brand, A.H., Schweisguth, F., 2010. Transcriptional control of stem cell maintenance in the Drosophila intestine. Development 137, 705–714. doi:10.1242/dev.039404

Barnett, D.W., Garrison, E.K., Quinlan, A.R., Strömberg, M.P., Marth, G.T., 2011. BamTools: a C++ API and toolkit for analyzing and managing BAM files. Bioinformatics 27, 1691–1692. doi:10.1093/bioinformatics/btr174

Beebe, K., Park, D., Taghert, P.H., Micchelli, C.A., 2015. The Drosophila Prosecretory Transcription Factor dimmed Is Dynamically Regulated in Adult Enteroendocrine Cells and Protects Against Gram-Negative Infection. G3 (Bethesda) 5, 1517–1524. doi:10.1534/g3.115.019117

Bertrand, N., Castro, D.S., Guillemot, F., 2002. Proneural genes and the specification of neural cell types. Nat Rev Neurosci 3, 517–530. doi:10.1038/nrn874

Bhattacharya, A., Baker, N.E., 2011. A Network of Broadly Expressed HLH Genes Regulates Tissue-Specific Cell Fates. Cell 147, 881–892. doi:10.1016/j.cell.2011.08.055

Bhattacharya, A., Baker, N.E., 2009. Developmental Biology. Developmental Biology 327, 288–300. doi:10.1016/j.ydbio.2008.11.037

Bischof, J., Duffraisse, M., Furger, E., Ajuria, L., Giraud, G., Vanderperre, S., Paul, R., Björklund, M., Ahr, D., Ahmed, A.W., Spinelli, L., Brun, C., Basler, K., Merabet, S.,

2018. Generation of a versatile BiFC ORFeome library for analyzing protein-protein interactions in live *Drosophila*. eLife 7. doi:10.7554/eLife.38853
Bray, S., Furriols, M., 2001. Notch pathway: Making sense of suppressor of hairless. Curr Biol 11, R217–R221. doi:10.1016/S0960-9822(01)00109-9
Brown, J.B., Boley, N., Eisman, R., May, G.E., Stoiber, M.H., Duff, M.O., Ben W Booth, Wen, J., Park, S., Suzuki, A.M., Wan, K.H., Yu, C., Zhang, D., Carlson, J.W., Cherbas, L., Eads, B.D., Miller, D., Mockaitis, K., Roberts, J., Davis, C.A., Frise, E., Hammonds, A.S., Olson, S., Shenker, S., Sturgill, D., Samsonova, A.A., Weiszmann, R., Robinson, G., Hernandez, J., Andrews, J., Bickel, P.J., Carninci, P., Cherbas, P., Gingeras, T.R., Hoskins, R.A., Kaufman, T.C., Lai, E.C., Oliver, B., Perrimon, N., Graveley, B.R., Celniker, S.E., 2014. Diversity and dynamics of the Drosophila transcriptome. Nature 512, 393–399. doi:10.1038/nature12962
Buchon, N., Osman, D., David, F.P.A., Fang, H.Y., Boquete, J.-P., Deplancke, B., Lemaitre, B., 2013. Morphological and molecular characterization of adult midgut compartmentalization in Drosophila. CellReports 3, 1725–1738. doi:10.1016/j.celrep.2013.04.001
Bundschuh, R., Hayot, F., Jayaprakash, C., 2003. The role of dimerization in noise reduction of simple genetic networks. J Theor Biol 220, 261–269. doi:10.1006/jtbi.2003.3164
Cabrera, C.V., Alonso, M.C., 1991. Transcriptional activation by heterodimers of the achaete-scute and daughterless gene products of Drosophila. EMBO J 10, 2965–2973.
Cabrera, C.V., Alonso, M.C., Huikeshoven, H., 1994. Regulation of scute function by extramacrochaete in vitro and in vivo. Development 120, 3595–3603.
Campuzano, S., 2001. Emc, a negative HLH regulator with multiple functions in Drosophila development. Oncogene 20, 8299–8307. doi:10.1038/sj.onc.1205162
Chen, J., Xu, N., Wang, C., Huang, P., Huang, H., Jin, Z., Yu, Z., Cai, T., Jiao, R., Xi, R., 2018. Transient Scute activation via a self-stimulatory loop directs enteroendocrine cell pair specification from self-renewing intestinal stem cells. Nature Cell Biology 20, 152–161. doi:10.1038/s41556-017-0020-0
Chintapalli, V.R., Wang, J., Dow, J.A.T., 2007. Using FlyAtlas to identify better Drosophila melanogaster models of human disease. Nat Genet 39, 715–720. doi:10.1038/ng2049
Cinquin, O., Demongeot, J., 2005. High-dimensional switches and the modelling of cellular differentiation. J Theor Biol 233, 391–411. doi:10.1016/j.jtbi.2004.10.027
Cinquin, O., Demongeot, J., 2002. Positive and negative feedback: Striking a balance between necessary antagonists. J Theor Biol 216, 229–241. doi:10.1006/jtbi.2002.2544
Crosnier, C., Stamataki, D., Lewis, J., 2006. Organizing cell renewal in the intestine: stem cells, signals and combinatorial control. Nat. Rev. Genet. 7, 349–359. doi:10.1038/nrg1840
Cubas, P., de Celis, J.F., Campuzano, S., Modolell, J., 1991. Proneural clusters of achaete-scute expression and the generation of sensory organs in the Drosophila imaginal wing disc. Genes & Development 5, 996–1008.
de Navascués, J., Perdigoto, C.N., Bian, Y., Schneider, M.H., Bardin, A.J., Martinez-Arias, A., Simons, B.D., 2012. Drosophila midgut homeostasis involves neutral competition between symmetrically dividing intestinal stem cells. EMBO J 31, 2473–2485. doi:10.1038/emboj.2012.106
Delidakis, C., Monastirioti, M., Magadi, S.S., 2014. E(spl): Genetic, Developmental, and Evolutionary Aspects of a Group of Invertebrate Hes Proteins with Close Ties to Notch Signaling. Current Topics in Developmental Biology: Transcriptional Switches During Development 110, 217–262. doi:10.1016/B978-0-12-405943-6.00006-3

Dobin, A., Davis, C.A., Schlesinger, F., Drenkow, J., Zaleski, C., Jha, S., Batut, P., Chaisson, M., Gingeras, T.R., 2013. STAR: ultrafast universal RNA-seq aligner. Bioinformatics 29, 15–21. doi:10.1093/bioinformatics/bts635

Doupé, D.P., Marshall, O.J., Dayton, H., Brand, A.H., Perrimon, N., 2018. Drosophila intestinal stem and progenitor cells are major sources and regulators of homeostatic niche signals. Proceedings of the National Academy of Sciences 115, 12218–12223. doi:10.1073/pnas.1719169115

Dutta, D., Dobson, A.J., Houtz, P.L., Gläßer, C., Revah, J., Korzelius, J., Patel, P.H., Edgar, B.A., Buchon, N., 2015. Regional Cell-Specific Transcriptome Mapping Reveals Regulatory Complexity in the Adult Drosophila Midgut. CellReports 1–14. doi:10.1016/j.celrep.2015.06.009

Dutta, D., Xiang, J., Edgar, B.A., 2013. RNA Expression Profiling from FACS-Isolated Cells of the Drosophila Intestine. Curr Protoc Stem Cell Biol 27, 2F.2.1–2F.2.12. doi:10.1002/9780470151808.sc02f02s27

D'Rozario, M., Zhang, T., Waddell, E.A., Zhang, Y., Sahin, C., Sharoni, M., Hu, T., Nayal, M., Kutty, K., Liebl, F., Hu, W., Marenda, D.R., 2016. Type I bHLH Proteins Daughterless and Tcf4 Restrict Neurite Branching and Synapse Formation by Repressing Neurexin in Postmitotic Neurons. CellReports 15, 386–397. doi:10.1016/j.celrep.2016.03.034

Ellis, H.M., 1994. Embryonic expression and function of the Drosophila helix-loop-helix gene, extramacrochaetae. Mech Dev 47, 65–72. doi:10.1016/0925-4773(94)90096-5

Engel, I., Murre, C., 2001. The function of E- and Id proteins in lymphocyte development. Nat Rev Immunol 1, 193–199. doi:10.1038/35105060

Fre, S., Huyghe, M., Mourikis, P., Robine, S., Louvard, D., Artavanis-Tsakonas, S., 2005. Notch signals control the fate of immature progenitor cells in the intestine. Nature Cell Biology 435, 964–968. doi:10.1038/nature03589

Furriols, M., Bray, S., 2001. A model Notch response element detects Suppressor of Hairless-dependent molecular switch. Curr Biol 11, 60–64.

Giot, L., Bader, J.S., Brouwer, C., Chaudhuri, A., Kuang, B., Li, Y., Hao, Y.L., Ooi, C.E., Godwin, B., Vitols, E., Vijayadamodar, G., Pochart, P., Machineni, H., Welsh, M., Kong, Y., Zerhusen, B., Malcolm, R., Varrone, Z., Collis, A., Minto, M., Burgess, S., McDaniel, L., Stimpson, E., Spriggs, F., Williams, J., Neurath, K., Ioime, N., Agee, M., Voss, E., Furtak, K., Renzulli, R., Aanensen, N., Carrolla, S., Bickelhaupt, E., Lazovatsky, Y., DaSilva, A., Zhong, J., Stanyon, C.A., Finley, R.L., White, K.P., Braverman, M., Jarvie, T., Gold, S., Leach, M., Knight, J., Shimkets, R.A., McKenna, M.P., Chant, J., Rothberg, J.M., 2003. A protein interaction map of Drosophila melanogaster. science (New York, NY) 302, 1727–1736. doi:10.1126/science.1090289

Graf, T., Enver, T., 2009. Forcing cells to change lineages. Nature 462, 587–594. doi:10.1038/nature08533

Guo, X., Huang, H., Yang, Z., Cai, T., Xi, R., 2019. Division of Labor: Roles of Groucho and CtBP in Notch-Mediated Lateral Inhibition that Controls Intestinal Stem Cell Differentiation in Drosophila. Stem Cell Reports 1–26. doi:10.1016/j.stemcr.2019.03.005

Guo, Z., Ohlstein, B., 2015. Bidirectional Notch signaling regulates Drosophila intestinal stem cell multipotency. science (New York, NY) 350, aab0988–aab0988. doi:10.1126/science.aab0988

Hartenstein, V., Takashima, S., Hartenstein, P., Asanad, S., Asanad, K., 2017. bHLH proneural genes as cell fate determinants of entero-endocrine cells, an evolutionarily conserved lineage sharing a common root with sensory neurons. Developmental Biology 431, 36–47. doi:10.1016/j.ydbio.2017.07.013

Hasskarl, J., Munger, K., 2014. Id Proteins - Tumor Markers or Oncogenes? Cancer Biol. Ther. 1, 91–96. doi:10.4161/cbt.50

Heinze, G., Ploner, M., Jiricka, L., Steiner, G., 2023. Firth's Bias-Reduced Logistic Regression [R package logistf version 1.25].
Herrmann, C., Van de Sande, B., Potier, D., Aerts, S., 2012. i-cisTarget: an integrative genomics method for the prediction of regulatory features and cis-regulatory modules. Nucleic Acids Res. 40, e114–e114. doi:10.1093/nar/gks543
Hinz, U., Giebel, B., Campos-Ortega, J.A., 1994. The Basic-Helix-Loop-Helix Domain of Drosophila Lethal of Scute Protein Is Sufficient for Proneural Function and Activates Neurogenic Genes. Cell 76, 77–87. doi:10.1016/0092-8674(94)90174-0
Horvay, K., Jarde, T., Casagranda, F., Perreau, V.M., Haigh, K., Nefzger, C.M., Akhtar, R., Gridley, T., Berx, G., Haigh, J.J., Barker, N., Polo, J.M., Hime, G.R., Abud, H.E., 2015. Snai1 regulates cell lineage allocation and stem cell maintenance in the mouse intestinal epithelium. EMBO J. doi:10.15252/embj.201490881
Hu, Y., Comjean, A., Perkins, L.A., Perrimon, N., Mohr, S.E., 2015. GLAD: an Online Database of Gene List Annotation for Drosophila. J. Genomics 3, 75–81. doi:10.7150/jgen.12863
Hung, R.-J., Hu, Y., Kirchner, R., Liu, Y., Xu, C., Comjean, A., Tattikota, S.G., Li, F., Song, W., Ho Sui, S., Perrimon, N., 2020. A cell atlas of the adult Drosophila midgut. Proceedings of the National Academy of Sciences 117, 1514–1523. doi:10.1073/pnas.1916820117
Jiang, H., Edgar, B.A., 2012. Intestinal stem cell function in Drosophila and mice. Curr. Opin. Genet. Dev. 1–7. doi:10.1016/j.gde.2012.04.002
Kanehisa, M., Furumichi, M., Sato, Y., Kawashima, M., Ishiguro-Watanabe, M., 2023. KEGG for taxonomy-based analysis of pathways and genomes. Nucleic Acids Res. 51, D587–D592. doi:10.1093/nar/gkac963
Korotkevich, G., Sukhov, V., Budin, N., Shpak, B., Artyomov, M.N., Sergushichev, A., 2021. Fast gene set enrichment analysis. bioRxiv 060012. doi:10.1101/060012
Korzelius, J., Naumann, S.K., Loza-Coll, M.A., Chan, J.S., Dutta, D., Oberheim, J., Gläßer, C., Southall, T.D., Brand, A.H., Jones, D.L., Edgar, B.A., 2014. Escargot maintains stemness and suppresses differentiation in Drosophila intestinal stem cells. EMBO J 33, 2967–2982. doi:10.15252/embj.201489072
Kunisch, M., Haenlin, M., Campos-Ortega, J.A., 1994. Lateral inhibition mediated by the Drosophila neurogenic gene delta is enhanced by proneural proteins. Proc Natl Acad Sci USA 91, 10139–10143. doi:10.1073/pnas.91.21.10139
Lan, Q., Cao, M., Kollipara, R.K., Rosa, J.B., Kittler, R., Jiang, H., 2018. FoxA transcription factor Fork head maintains the intestinal stem/progenitor cell identities in Drosophila. Developmental Biology 433, 324–343. doi:10.1016/j.ydbio.2017.09.002
Lee, T., Luo, L., 1999. Mosaic analysis with a repressible cell marker for studies of gene function in neuronal morphogenesis. Neuron 22, 451–461.
Levine, M., Davidson, E.H., 2005. Gene regulatory networks for development. Proc Natl Acad Sci USA 102, 4936–4942. doi:10.1073/pnas.0408031102
Li, H., Janssens, J., De Waegeneer, M., Kolluru, S.S., Davie, K., Gardeux, V., Saelens, W., David, F.P.A., Brbić, M., Spanier, K., Leskovec, J., McLaughlin, C.N., Xie, Q., Jones, R.C., Brueckner, K., Shim, J., Tattikota, S.G., Schnorrer, F., Rust, K., Nystul, T.G., Carvalho-Santos, Z., Ribeiro, C., Pal, S., Mahadevaraju, S., Przytycka, T.M., Allen, A.M., Goodwin, S.F., Berry, C.W., Fuller, M.T., White-Cooper, H., Matunis, E.L., DiNardo, S., Galenza, A., O'Brien, L.E., Dow, J.A.T., FCA Consortium§, Jasper, H., Oliver, B., Perrimon, N., Deplancke, B., Quake, S.R., Luo, L., Aerts, S., Agarwal, D., Ahmed-Braimah, Y., Arbeitman, M., Ariss, M.M., Augsburger, J., Ayush, K., Baker, C.C., Banisch, T., Birker, K., Bodmer, R., Bolival, B., Brantley, S.E., Brill, J.A., Brown, N.C., Buehner, N.A., Cai, X.T., Cardoso-Figueiredo, R., Casares, F., Chang, A., Clandinin, T.R., Crasta, S., Desplan, C., Detweiler, A.M., Dhakan, D.B., Donà, E., Engert, S., Floc'hlay, S., George, N., González-Segarra, A.J., Groves, A.K., Gumbin, S., Guo, Y., Harris, D.E., Heifetz, Y., Holtz, S.L., Horns, F., Hudry, B., Hung, R.-J., Jan, Y.N.,

Jaszczak, J.S., Jefferis, G.S.X.E., Karkanias, J., Karr, T.L., Katheder, N.S., Kezos, J., Kim, A.A., Kim, S.K., Kockel, L., Konstantinides, N., Kornberg, T.B., Krause, H.M., Labott, A.T., Laturney, M., Lehmann, R., Leinwand, S., Li, J., Li, J.S.S., Li, K., Li, K., Li, L., Li, T., Litovchenko, M., Liu, H.-H., Liu, Y., Lu, T.-C., Manning, J., Mase, A., Matera-Vatnick, M., Matias, N.R., McDonough-Goldstein, C.E., McGeever, A., McLachlan, A.D., Moreno-Roman, P., Neff, N., Neville, M., Ngo, S., Nielsen, T., O'Brien, C.E., Osumi-Sutherland, D., Özel, M.N., Papatheodorou, I., Petkovic, M., Pilgrim, C., Pisco, A.O., Reisenman, C., Sanders, E.N., Santos, Dos, G., Scott, K., Sherlekar, A., Shiu, P., Sims, D., Sit, R.V., Slaidina, M., Smith, H.E., Sterne, G., Su, Y.-H., Sutton, D., Tamayo, M., Tan, M., Tastekin, I., Treiber, C., Vacek, D., Vogler, G., Waddell, S., Wang, W., Wilson, R.I., Wolfner, M.F., Wong, Y.-C.E., Xie, A., Xu, J., Yamamoto, S., Yan, J., Yao, Z., Yoda, K., Zhu, R., Zinzen, R.P., 2022. Fly Cell Atlas: A single-nucleus transcriptomic atlas of the adult fruit fly. science (New York, NY) 375, eabk2432. doi:10.1126/science.abk2432

Li, K., Baker, N.E., 2019. Transcriptional and post-transcriptional regulation of extra macrochaetae during Drosophila adult peripheral neurogenesis. Developmental Biology 449, 41–51. doi:10.1016/j.ydbio.2019.02.003

Li, K., Baker, N.E., 2018. Regulation of the Drosophila ID protein Extra macrochaetae by proneural dimerization partners. eLife 7. doi:10.7554/eLife.33967

Li, Y., Pang, Z., Huang, H., Wang, C., Cai, T., Xi, R., 2017. Transcription Factor Antagonism Controls Enteroendocrine Cell Specification from Intestinal Stem Cells. Sci Rep 7, 988. doi:10.1038/s41598-017-01138-z

Liao, Y., Smyth, G.K., Shi, W., 2014. featureCounts: an efficient general purpose program for assigning sequence reads to genomic features. Bioinformatics 30, 923–930. doi:10.1093/bioinformatics/btt656

Love, M.I., Huber, W., Anders, S., 2014. Moderated estimation of fold change and dispersion for RNA-seq data with DESeq2. Genome Biol 15, 550. doi:10.1186/s13059-014-0550-8

Lowe, N., Rees, J.S., Roote, J., Ryder, E., Armean, I.M., Johnson, G., Drummond, E., Spriggs, H., Drummond, J., Magbanua, J.P., Naylor, H., Sanson, B., Bastock, R., Huelsmann, S., Trovisco, V., Landgraf, M., Knowles-Barley, S., Armstrong, J.D., White-Cooper, H., Hansen, C., Phillips, R.G., UK Drosophila Protein Trap Screening Consortium, Lilley, K.S., Russell, S., St Johnston, D., 2014. Analysis of the expression patterns, subcellular localisations and interaction partners of Drosophila proteins using a pigP protein trap library. Development 141, 3994–4005. doi:10.1242/dev.111054

Loza-Coll, M.A., Southall, T.D., Sandall, S.L., Brand, A.H., Jones, D.L., 2014. Regulation of Drosophila intestinal stem cell maintenance and differentiation by the transcription factor Escargot. EMBO J 33, 2983–2996. doi:10.15252/embj.201489050

Malaguti, M., Migueles, R.P., Blin, G., Lin, C.-Y., Lowell, S., 2019. Id1 Stabilizes Epiblast Identity by Sensing Delays in Nodal Activation and Adjusting the Timing of Differentiation. Dev Cell 1–22. doi:10.1016/j.devcel.2019.05.032

Marianes, A., Spradling, A.C., 2013. Author response. eLife 2, 155–19. doi:10.7554/eLife.00886

Massari, M.E., Murre, C., 2000. Helix-loop-helix proteins: regulators of transcription in eucaryotic organisms. Molecular and Cellular Biology 20, 429–440.

Micchelli, C.A., Perrimon, N., 2006. Evidence that stem cells reside in the adult Drosophila midgut epithelium. Nature 439, 475–479. doi:10.1038/nature04371

Moore, A.W., Barbel, S., Jan, L.Y., Jan, Y.N., 2000. A genomewide survey of basic helix-loop-helix factors in Drosophila. Proc Natl Acad Sci USA 97, 10436–10441. doi:10.1073/pnas.170301897

Moris, N., Pina, C., Arias, A.M., 2016. Transition states and cell fate decisions in epigenetic landscapes. Nat. Rev. Genet. 17, 693–703. doi:10.1038/nrg.2016.98

Murre, C., 2005. Helix-loop-helix proteins and lymphocyte development. Nat Immunol 6, 1079–1086. doi:10.1038/ni1260
Murre, C., Bain, G., VANDIJK, M.A., Engel, I., Furnari, B.A., Massari, M.E., Matthews, J.R., Quong, M.W., Rivera, R.R., Stuiver, M.H., 1994. Structure and Function of Helix-Loop-Helix Proteins. Biochim Biophys Acta 1218, 129–135. doi:10.1016/0167-4781(94)90001-9
Neuhold, L.A., Wold, B., 1993. HLH forced dimers: Tethering MyoD to E47 generates a dominant positive myogenic factor insulated from negative regulation by Id. Cell 74, 1033–1042. doi:10.1016/0092-8674(93)90725-6
Norton, J.D., 2000. ID helix-loop-helix proteins in cell growth, differentiation and tumorigenesis. J Cell Sci 113 (Pt 22), 3897–3905.
Ohlstein, B., Spradling, A., 2007. Multipotent Drosophila intestinal stem cells specify daughter cell fates by differential notch signaling. science (New York, NY) 315, 988–992. doi:10.1126/science.1136606
Ohlstein, B., Spradling, A., 2006. The adult Drosophila posterior midgut is maintained by pluripotent stem cells. Nature 439, 470–474. doi:10.1038/nature04333
Okumura, T., Takeda, K., Kuchiki, M., Akaishi, M., Taniguchi, K., Adachi-Yamada, T., 2016. GATAe regulates intestinal stem cell maintenance and differentiation in Drosophila adult midgut. Developmental Biology 410, 24–35. doi:10.1016/j.ydbio.2015.12.017
Patel, P.H., Dutta, D., Edgar, B.A., 2015. Niche appropriation by Drosophila intestinal stem cell tumours. Nature Cell Biology 17, 1182–1192. doi:10.1038/ncb3214
Philpott, A., Winton, D.J., 2014. Lineage selection and plasticity in the intestinal crypt. Curr Opin Cell Biol 31, 39–45. doi:10.1016/j.ceb.2014.07.002
R Core Team, 2023. R: A Language and Environment for Statistical Computing. Vienna, Austria.
Resende, L.P.F., Truong, M.E., Gomez, A., Jones, D.L., 2017. Intestinal stem cell ablation reveals differential requirements for survival in response to chemical challenge. Developmental Biology 424, 10–17. doi:10.1016/j.ydbio.2017.01.004
Ritchie, M.E., Phipson, B., Wu, D., Hu, Y., Law, C.W., Shi, W., Smyth, G.K., 2015. limma powers differential expression analyses for RNA-sequencing and microarray studies. Nucleic Acids Res. 43, e47. doi:10.1093/nar/gkv007
Sallee, M.D., Littleford, H.E., Greenwald, I., 2017. A bHLH Code for Sexually Dimorphic Form and Function of the C. elegans Somatic Gonad. Curr Biol 27, 1853–1860.e5. doi:10.1016/j.cub.2017.05.059
Schindelin, J., Arganda-Carreras, I., Frise, E., Kaynig, V., Longair, M., Pietzsch, T., Preibisch, S., Rueden, C., Saalfeld, S., Schmid, B., Tinevez, J.-Y., White, D.J., Hartenstein, V., Eliceiri, K., Tomancak, P., Cardona, A., 2012. Fiji: an open-source platform for biological-image analysis. Nat Methods 9, 676–682. doi:10.1038/nmeth.2019
Shokri, L., Inukai, S., Hafner, A., Weinand, K., Hens, K., Vedenko, A., Gisselbrecht, S.S., Dainese, R., Bischof, J., Furger, E., Feuz, J.-D., Basler, K., Deplancke, B., Bulyk, M.L., 2019. A Comprehensive Drosophila melanogaster Transcription Factor Interactome. cell reports 27, 955–970.e7. doi:10.1016/j.celrep.2019.03.071
Simon, C.S., Hadjantonakis, A.-K., Schröter, C., 2018. Making lineage decisions with biological noise: Lessons from the early mouse embryo. WIREs Dev Biol 7, e319–16. doi:10.1002/wdev.319
Siudeja, K., Nassari, S., Gervais, L., Skorski, P., Lameiras, S., Stolfa, D., Zande, M., Bernard, V., Frio, T.R., Bardin, A.J., 2015. Frequent Somatic Mutation in Adult Intestinal Stem Cells Drives Neoplasia and Genetic Mosaicism during Aging. Cell Stem Cell 17, 663–674. doi:10.1016/j.stem.2015.09.016
Spratford, C.M., Kumar, J.P., 2015. Inhibition of Daughterless by Extramacrochaetae mediates Notch-induced cell proliferation. Development 142, 2058–2068. doi:10.1242/dev.121855

Street, K., Risso, D., Fletcher, R.B., Das, D., Ngai, J., Yosef, N., Purdom, E., Dudoit, S., 2018. Slingshot: cell lineage and pseudotime inference for single-cell transcriptomics. BMC Genomics 19, 477–16. doi:10.1186/s12864-018-4772-0

Subramanian, A., Tamayo, P., Mootha, V.K., Mukherjee, S., Ebert, B.L., Gillette, M.A., Paulovich, A., Pomeroy, S.L., Golub, T.R., Lander, E.S., Mesirov, J.P., 2005. Gene set enrichment analysis: A knowledge-based approach for interpreting genome-wide expression profiles. Proc Natl Acad Sci USA 102, 15545–15550. doi:10.1073/pnas.0506580102

Tanaka-Matakatsu, M., Miller, J., Borger, D., Tang, W.-J., Du, W., 2014. Daughterless homodimer synergizes with Eyeless to induce Atonal expression and retinal neuron differentiation. Developmental Biology 392, 256–265. doi:10.1016/j.ydbio.2014.05.019

Tapanes-Castillo, A., Baylies, M.K., 2004. Notch signaling patterns Drosophila mesodermal segments by regulating the bHLH transcription factor twist. Development 131, 2359–2372. doi:10.1242/dev.01113

Tetteh, P.W., Basak, O., Farin, H.F., Wiebrands, K., Kretzschmar, K., Begthel, H., van den Born, M., Korving, J., de Sauvage, F., van Es, J.H., van Oudenaarden, A., Clevers, H., 2016. Replacement of Lost Lgr5-Positive Stem Cells through Plasticity of Their Enterocyte-Lineage Daughters. Cell Stem Cell 18, 203–213. doi:10.1016/j.stem.2016.01.001

Troost, T., Schneider, M., Klein, T., 2015. A re-examination of the selection of the sensory organ precursor of the bristle sensilla of Drosophila melanogaster. PLoS Genet 11, e1004911. doi:10.1371/journal.pgen.1004911

van der Flier, L.G., van Gijn, M.E., Hatzis, P., Kujala, P., Haegebarth, A., Stange, D.E., Begthel, H., van den Born, M., Guryev, V., Oving, I., van Es, J.H., Barker, N., Peters, P.J., van de Wetering, M., Clevers, H., 2009. Transcription factor achaete scute-like 2 controls intestinal stem cell fate. Cell 136, 903–912. doi:10.1016/j.cell.2009.01.031

Van Doren, M., Ellis, H.M., Posakony, J.W., 1991. The Drosophila extramacrochaetae protein antagonizes sequence-specific DNA binding by daughterless/achaete-scute protein complexes. Development 113, 245–255.

van Es, J.H., van Gijn, M.E., Riccio, O., van den Born, M., Vooijs, M., Begthel, H., Cozijnsen, M., Robine, S., Winton, D.J., Radtke, F., Clevers, H., 2005. Notch/γ-secretase inhibition turns proliferative cells in intestinal crypts and adenomas into goblet cells. Nature Cell Biology 435, 959–963. doi:10.1038/nature03659

Wang, C., Guo, X., Dou, K., Chen, H., Xi, R., 2015. Ttk69 acts as a master repressor of enteroendocrine cell specification in Drosophila intestinal stem cell lineages. Development 142, 3321–3331. doi:10.1242/dev.123208

Wang, L.-H., Baker, N.E., 2015. E Proteins and ID Proteins: Helix-Loop-Helix Partners in Development and Disease. Dev Cell 35, 269–280. doi:10.1016/j.devcel.2015.10.019

Wice, B.M., 1998. Forced Expression of Id-1 in the Adult Mouse Small Intestinal Epithelium Is Associated with Development of Adenomas. Journal of Biological Chemistry 273, 25310–25319. doi:10.1074/jbc.273.39.25310

Yin, C., Xi, R., 2018. A Phyllopod-Mediated Feedback Loop Promotes Intestinal Stem Cell Enteroendocrine Commitment in Drosophila. Stem Cell Reports 10, 43–57. doi:10.1016/j.stemcr.2017.11.014

Zeng, X., Chauhan, C., Hou, S.X., 2010. Characterization of midgut stem cell- and enteroblast-specific Gal4 lines in drosophila. Genesis 48, 607–611. doi:10.1002/dvg.20661

Zeng, X., Hou, S.X., 2015. Enteroendocrine cells are generated from stem cells through a distinct progenitor in the adult Drosophila posterior midgut. Development 142, 644–653. doi:10.1242/dev.113357

Zhai, Z., Kondo, S., Ha, N., Boquete, J.-P., Brunner, M., Ueda, R., Lemaitre, B., 2015. Accumulation of differentiating intestinal stem cell progenies drives tumorigenesis. Nat Commun 6, 10219–27. doi:10.1038/ncomms10219

Zhang, C., Jin, Y., Marchetti, M., Lewis, M.R., Hammouda, O.T., Edgar, B.A., 2022. EGFR signaling activates intestinal stem cells by promoting mitochondrial biogenesis and β-oxidation. Curr Biol 32, 3704–3719.e7. doi:10.1016/j.cub.2022.07.003

Zhang, N., Yantiss, R.K., Nam, H.-S., Chin, Y., Zhou, X.K., Scherl, E.J., Bosworth, B.P., Subbaramaiah, K., Dannenberg, A.J., Benezra, R., 2014. ID1 Is a Functional Marker for Intestinal Stem and Progenitor Cells Required for Normal Response to Injury. Stem Cell Reports 3, 716–724. doi:10.1016/j.stemcr.2014.09.012

Figure 1 Puig-Barbe et al., 2023

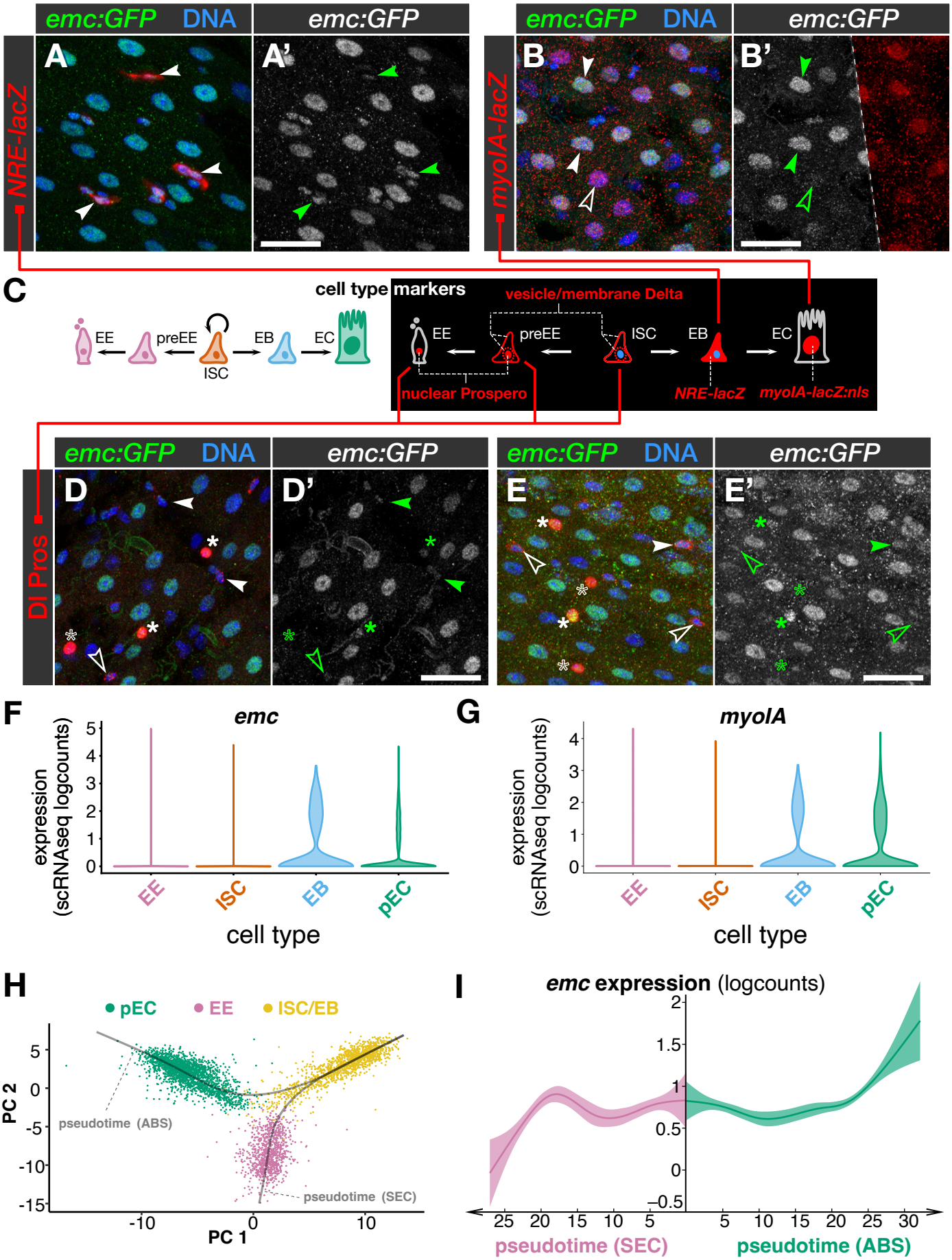

(from the previous page)

Figure 1. *emc* is expressed preferentially in the absorptive lineage.
A-E. Projected confocal stacks (A-B, D-E) showing endogenous Emc:GFP expression, and schematic illustrating the ISC lineage and our usage of cell type markers (C): ISCs are recognised by Dl expression; EEs by Prospero; EBs by NRE-lacZ; ECs by *myoIA-lacZ* and being polyploid. Emc is expressed in EBs (marked with *NRE-lacZ*, arrowheads in A, A') and most ECs (positive for *myoIA-lacZ*, solid arrowheads in B, B') but not all (empty arrowhead in B, B'). *emc* expression can also be detected in some ISCs (Dl^+) and EEs ($Pros^+$) (solid arrowheads and asterisks, respectively, in C-D') but not all (empty arrowheads and asterisks in C-D'). Scale bars: 20μm. **F, G.** Expression of *emc* (E) and the EC marker *myoIA* (F) by scRNAseq in EEs, ISCs, EBs and ECs from the posterior midgut (pECs). Both genes are enriched in EBs and ECs, with rare events of detection in EEs and ISCs. **H.** Pseudotime trajectories from ISC/EB cells into mature EEs or ECs derived from scRNAseq data. **I.** *emc* expression in single cells declines as these get closer to the EE fate and increases as they progress towards EC differentiation.

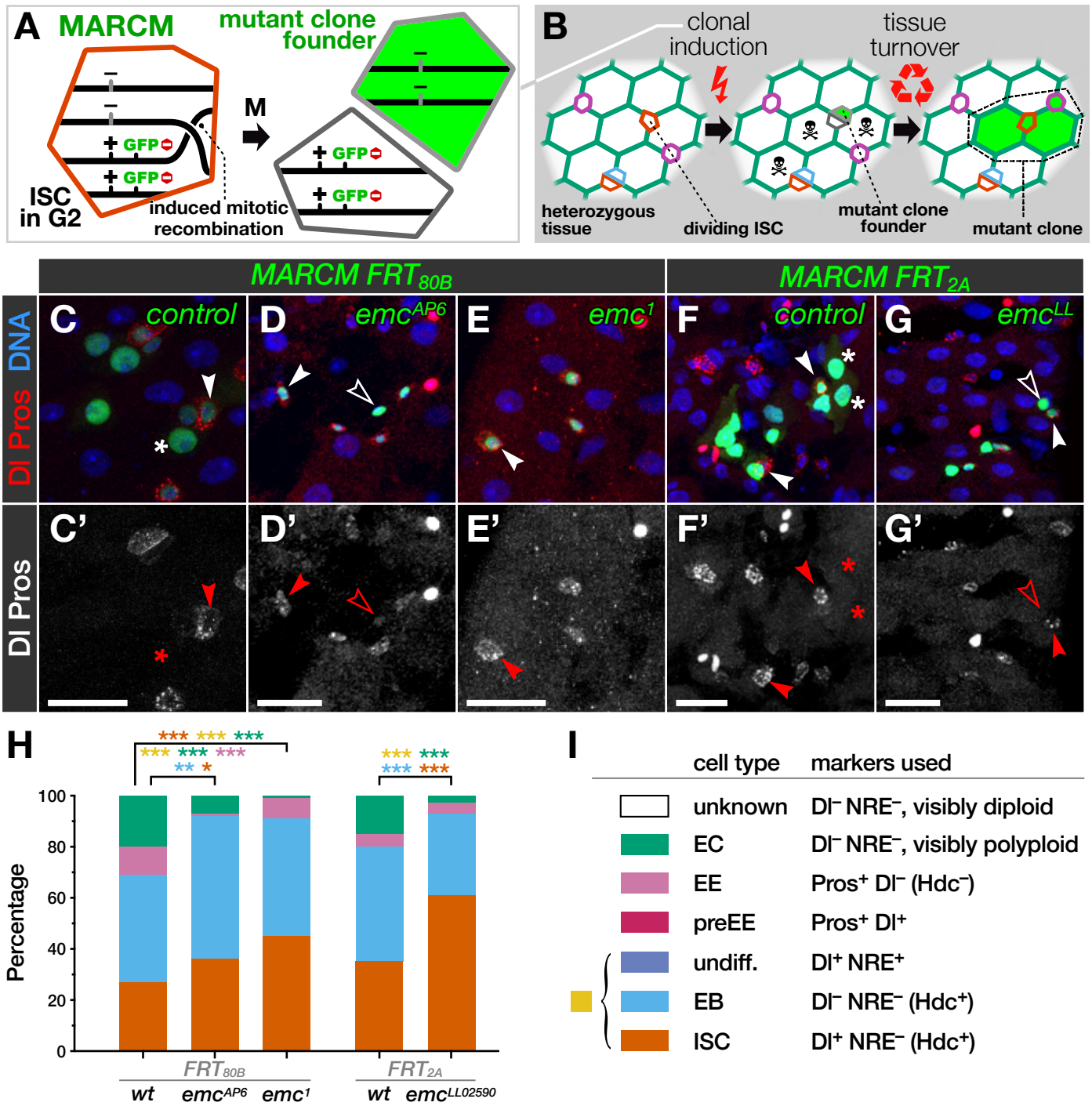

Figure 2. *emc* is necessary for differentiation.
A-B. MARCM method: the FRT-FLP system is used to induce mitotic recombination in G2, which during mitosis (M) can result in co-segregation of sister chromatid arms (A). (B) After clonal induction, a subset of ISCs generate sparse labelled clones that can be followed up as tissue turns over. **C-G.** Differentiation is impaired in *emc* mutant clones. Control clones display more polyploid Dl⁻/Pros⁻ ECs (asterisks in C, F) than clones homozygous of for the mutant alleles emc^{AP6} (D), emc^{1} (E) and $emc^{LL02590}$ (G), which are enriched in Dl⁺ ISCs (solid arrowheads) and diploid Dl⁻/Pros⁻ EBs (empty arrowheads) with respect to controls. **H.** Stacked bars plots aggregating cell type composition of MARCM clones shown in C-G. Numbers (cells/clones): control *FRT80B*, 310/117; emc^{1}, 112/95, emc^{AP6}, 208/200; control *FRT2A*, 194/106; $emc^{LL02590}$, 213/118. *p*-values are <0.05, <0.01 and <0.001 for one, two or three asterisks (see Tables S1 and S2 for further details). **I.** Types of cells considered in this work, with their colour representation and the markers used for their classification throughout the paper. Scale bars: 20μm.

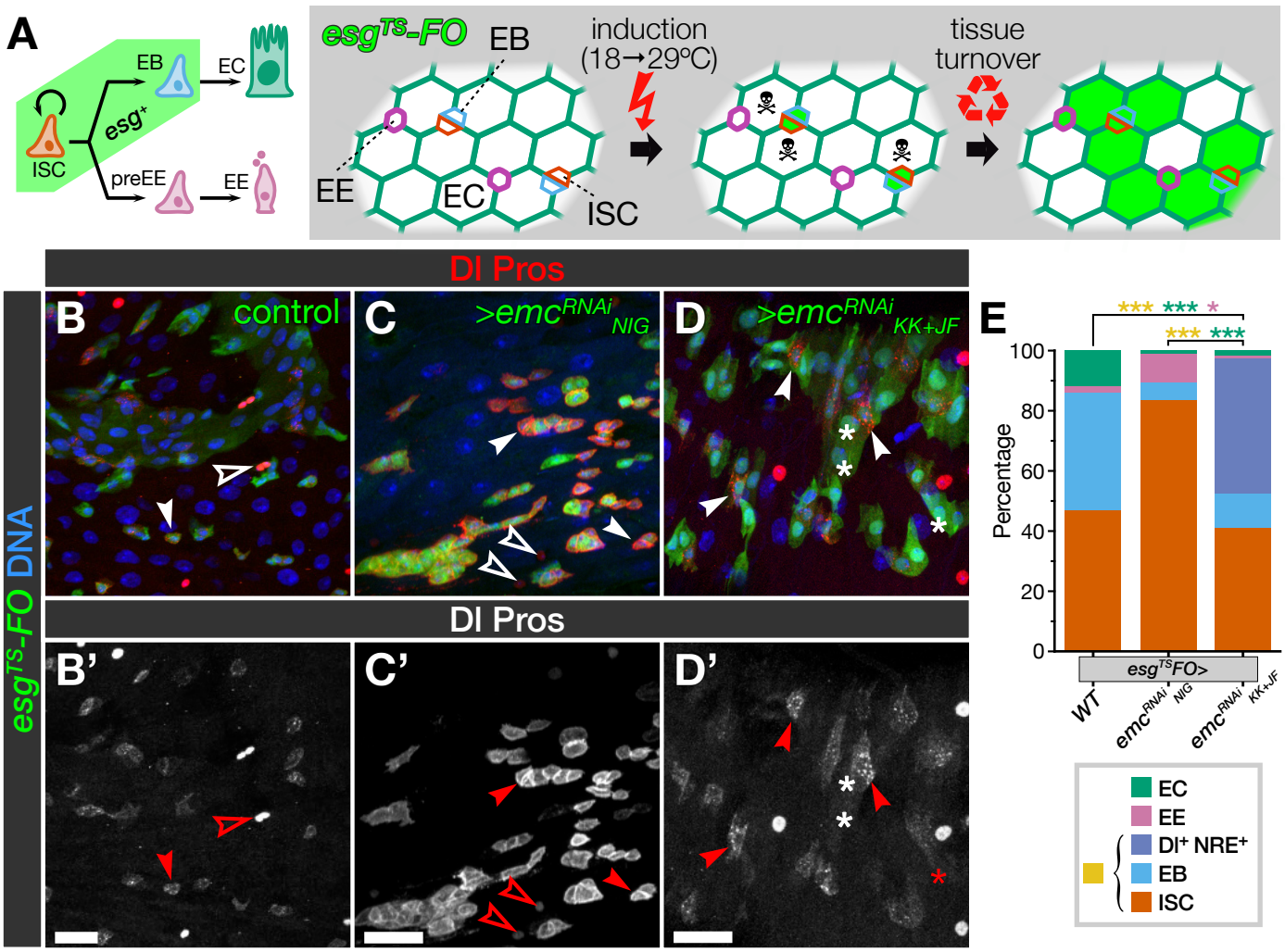

Figure 3. *emc* is required for differentiation into mature ECs.
A. Use of the *esg*^{TS}*-FO* system allows the simultaneous manipulation and tracing of ISCs and EBs. *esg-Gal4, UAS-GFP* is expressed specifically in ISCs/EBs after induction (left panel) and activates irreversibly in ISCs/EBs the ubiquitous *Actin5C-Gal4*, which in turn will maintain *UAS-GFP* expression if differentiation or commitment occur (right panel). **B-D.** ISCs and EBs in *esg*^{TS}*-FO* control guts produce both EC (Dl$^-$/Pros$^-$) and EE (Dl$^-$/Pros$^+$) GFP$^+$ cells (B, note the difference in intensity levels between Dl and Pros, solid and empty arrowheads, respectively); differentiation is reduced when ISCs/EBs express *emc*-specific RNAi, shown by increased number of Dl$^+$/GFP$^+$ cells (C, D). Reduction of *emc* also induces increased Dl expression: compare Dl-expressing with Pros-expressing cells (respectively solid and empty arrowheads in C, D), with those similarly marked in B. **F.** Stacked bars plots aggregating the cell type composition of *esg*^{TS}*-FO* tissue from B-E. Numbers (total GFP$^+$ cells / fields of view): control, 1046/15; *UAS-emc*$^{RNAi}_{NIG}$, 104/21; *UAS-emc*$^{RNAi}_{KK+HMS}$, 832/15. p-values are <0.05, <0.01 and <0.001 for one, two or three asterisks (see Tables S1 and S2). Scale bars: 20μm.

Figure 4 Puig-Barbe et al., 2023

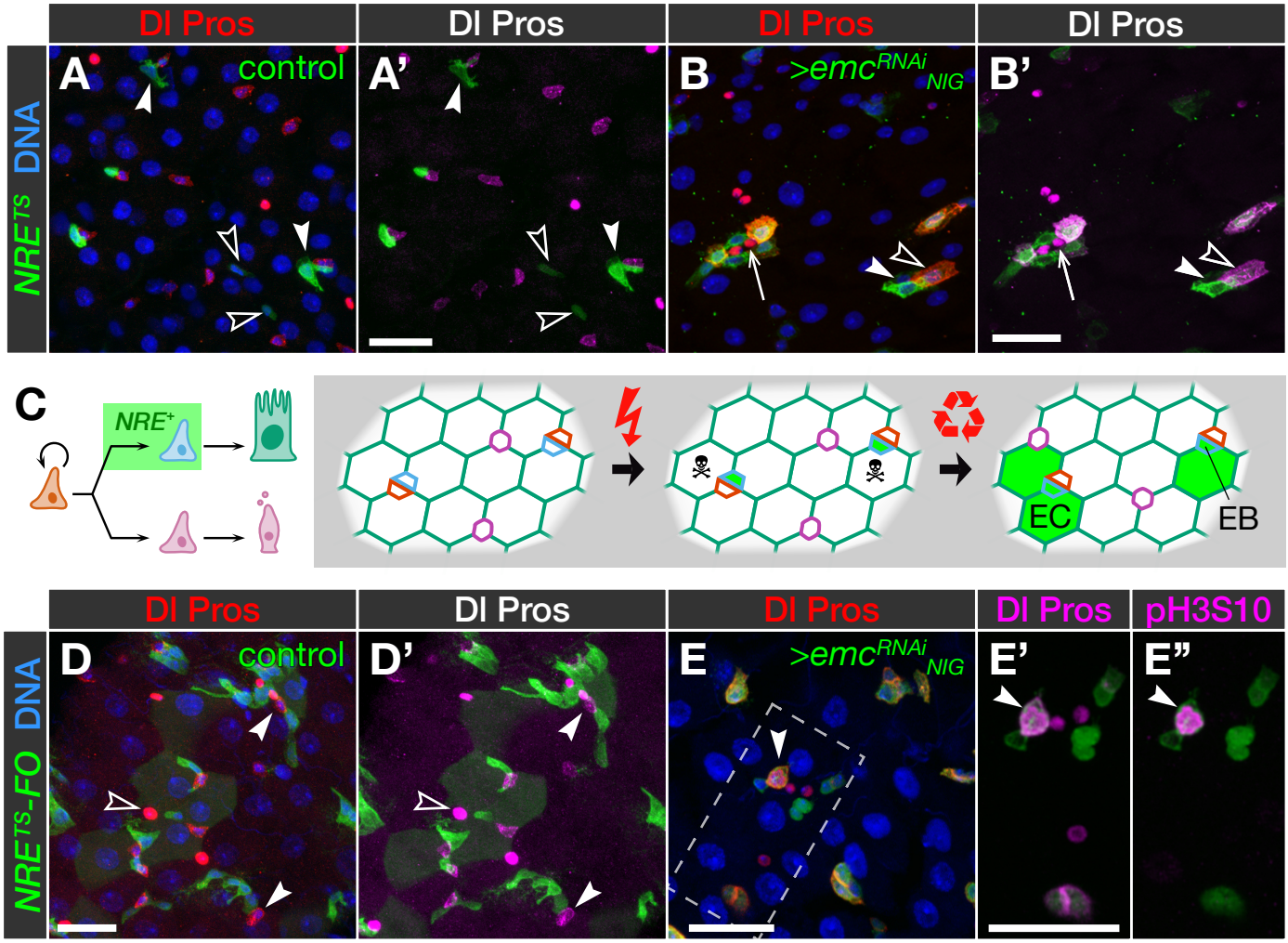

Figure 4. *emc* is required for maintenance of the EB committed state.
A-B. The *NRE-Gal4* driver is expressed in EBs at different levels in normal intestines (solid and empty arrowheads in A for higher and lower-expressing EBs), but never co-express Dl. When *emc* is depleted with *NRE-Gal4*, many EBs co-express Dl (empty arrowheads, B) but not all (solid arrowheads, B). Also, EEs develop close to *emc*-depleted EBs (arrow, B). **C.** Use of *NRE^{TS}-FO* allows the simultaneous manipulation and tracing of the EB lineage. *NRE-Gal4, UAS-GFP* is expressed specifically in EBs after induction (left panel) and activates irreversibly in EBs the ubiquitous *Actin5C-Gal4*, which in turn will maintain *UAS-GFP* expression if differentiation or decommitment occur (right panel). **D-E**. Loss of *emc* in EBs leads to their decommitment. Activation of *NRE^{TS}-FO* in control guts leads exclusively to the labelling of EBs and ECs, with no co-expression of GFP and Dl or Pros (solid and empty arrowheads, respectively, in D; some ISCs and EEs in the micrograph seem inside the GFP territory due to the Z-projection of the confocal stack). By contrast, in *NRE^{TS}-FO* guts where *emc* is depleted, EB-derived cells express Dl and are capable of mitosis, as judged by phospho-Histone H3S10 staining (arrowhead in E-E"). Scale bars: 20μm.

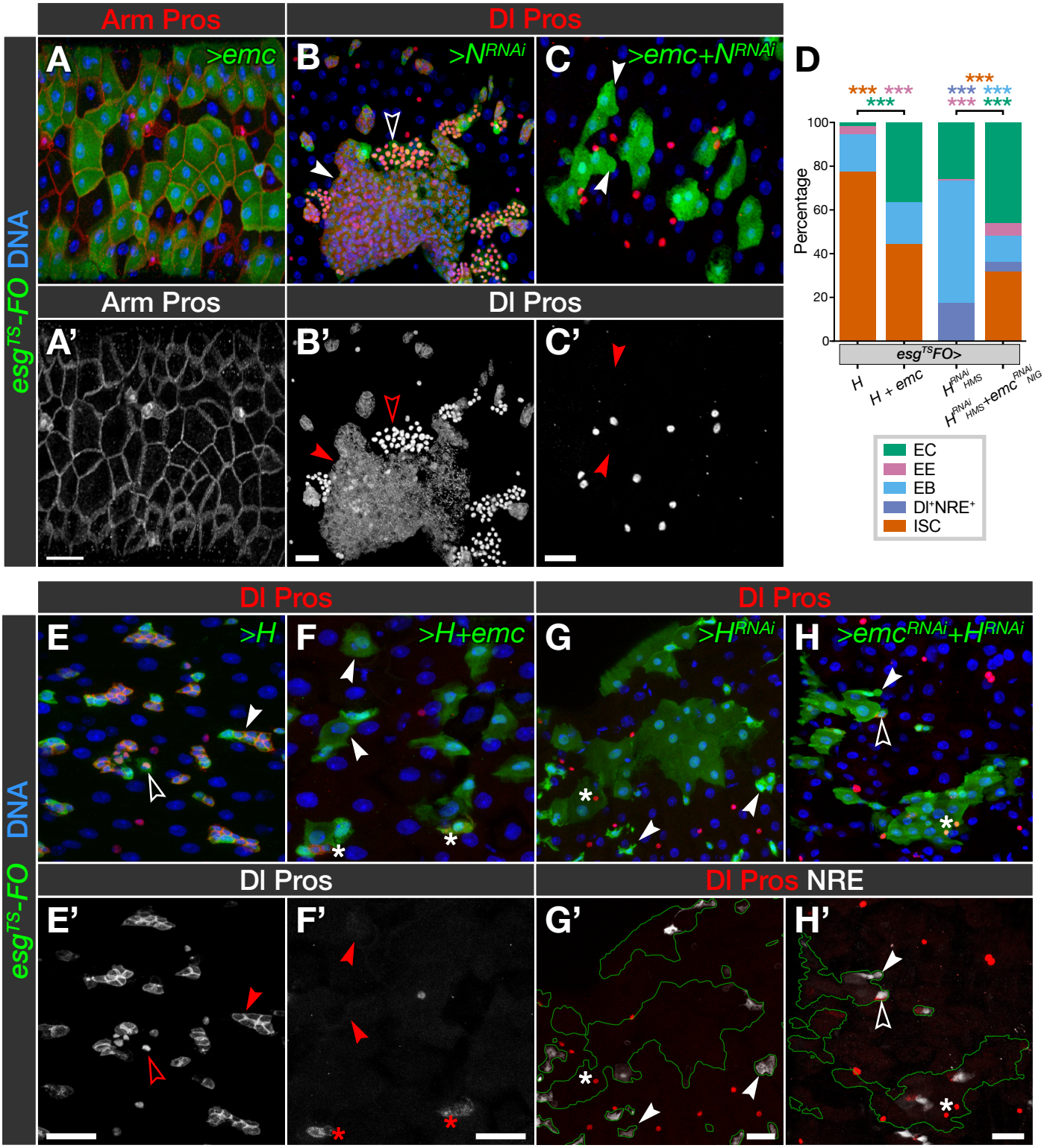

Figure 5. *emc* induces EC differentiation in parallel to Notch signalling.
A. Forced expression of *emc* in ISCs/EBs induces differentiation into ECs: 99.4% of GFP⁺ were ECs; ISCs, EBs and EEs were 0.2, 0.2 and 0.4%, respectively; data from 812 cells from 10 fields of view). **B.** EC differentiation is abolished with knockdown of *N*, where there is accumulation of Dl⁺ (solid arrowheads) or Pros⁺ (empty arrowheads) cells. **C.** Simultaneous knockdown of *N* with overexpression of *emc* induces EC differentiation (arrowheads). **D.** Stacked bars plots aggregating the cell type composition of *esg*^{TS}*-FO* tissue from E-H. Numbers (total GFP⁺ cells / fields of view): *UAS-H*, 1810/21; *UAS-H+UAS-emc*, 1292/27; *UAS-H*$^{RNAi}_{HMS}$, 984/15; *UAS-H*$^{RNAi}_{HMS}$*+UAS-emc*$^{RNAi}_{NIG}$, 126/16. p-values are <0.05, <0.01 and <0.001 for one, two or three asterisks (see Tables S1 and S2). **E-F.** Overexpression of *H* strongly impairs EC differentiation and leads to accumulation of Dl⁺ (solid arrowheads) or Pros⁺ (empty arrowheads) cells (E). Simultaneous overexpression *emc* induces EC differentiation (F), but to a lesser an extent than in the background of *N* knockdown (asterisks in F, compare with C). **G-H.** Depletion of *H* induces EC differentiation (G) even in the absence of *emc* (G, D). Scale bars: 20μm.

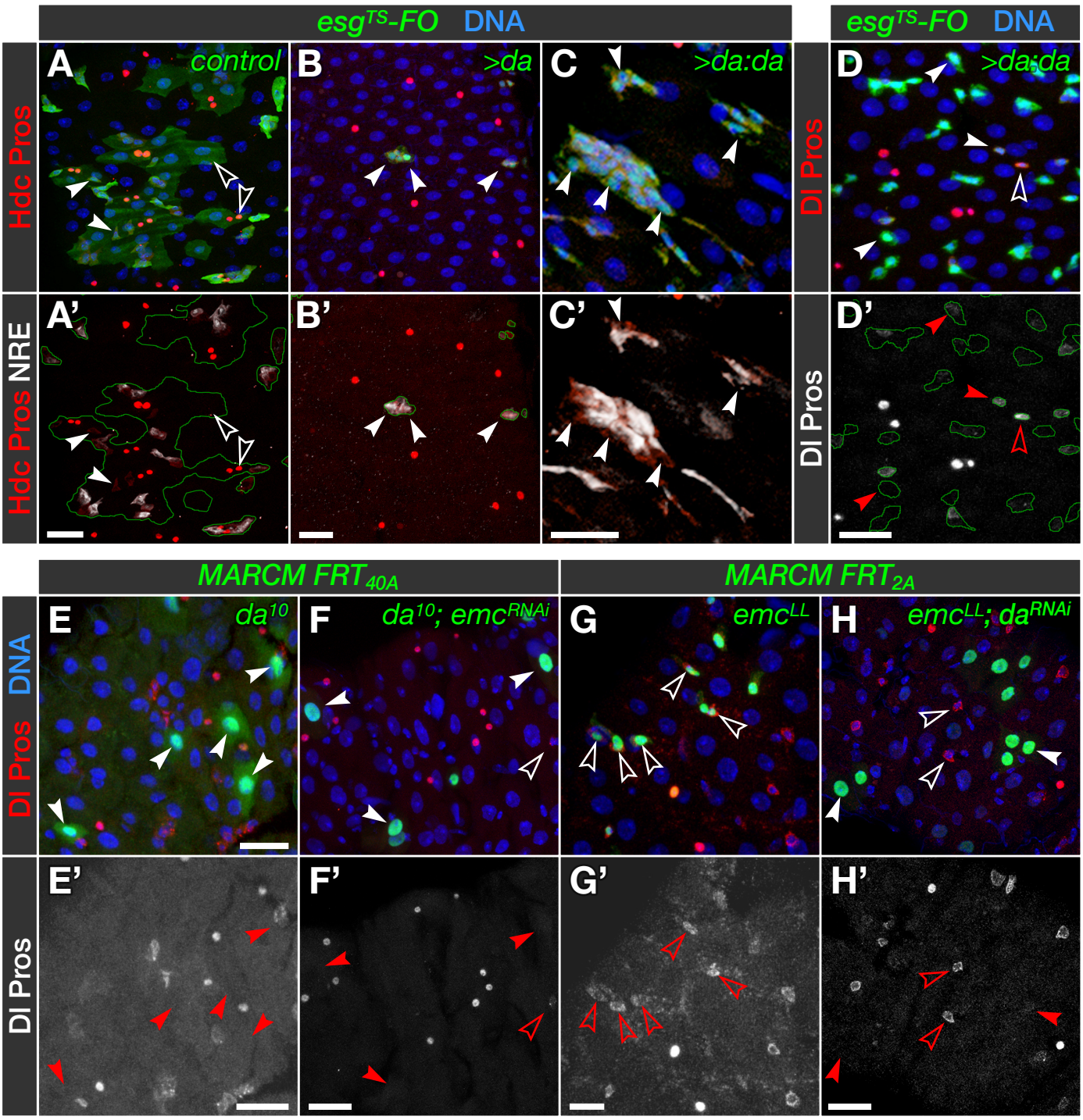

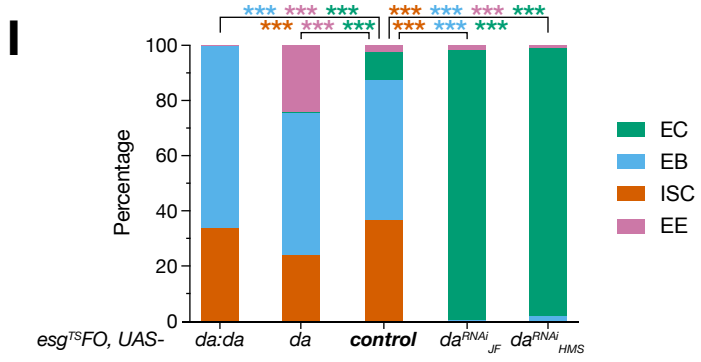

Figure 6. Da homodimers prevent differentiation and are antagonised by Emc.
A-D. Da homodimers maintain ISCs/EBs undifferentiated. Solid arrowheads: ISCs/EBs; empty arrowheads: ECs/EEs. Overexpression of Da with *esg*^{TS}*-FO* prevents formation of ECs, though it allows EE differentiation (B, compare with A). Expression of a forced Da:Da dimer in esg^{+} cells prevents all differentiation, as evaluated with Hdc/NRE-lacZ (C) or Dl (D). **E-H.** *da* is epistatic over *emc*. Solid arrowheads: ECs; empty arrowheads: Dl^{+} ISCs. MARCM clones mutant for *da*^{10} differentiate as ECs (E). This phenotype is recapitulated when these clones simultaneously express *emc*-specific RNAi (F). Likewise, impaired differentiation in *emc*^{LL02590} clones (G) is rescued by simultaneous knockdown of *da*, which leads to EC formation (H). **I.** Stacked bars plots summarising the cell type composition of *esg*^{TS}*-FO* tissue. Numbers (total GFP^{+} cells / fields of view) are 1135/15, 549/14, 693/13, 803/15 and 1086/19 for control, *UAS-da*, *UAS-da:da*, *UAS-da*$^{RNAi}_{JF}$ and *UAS-da*$^{RNAi}_{HMS}$, respectively. P-values are <0.05, <0.01 and <0.001 for one, two or three asterisks (see Tables S1 and S2). Scale bars: 20μm.

Figure 7

Puig-Barbe et al., 2023

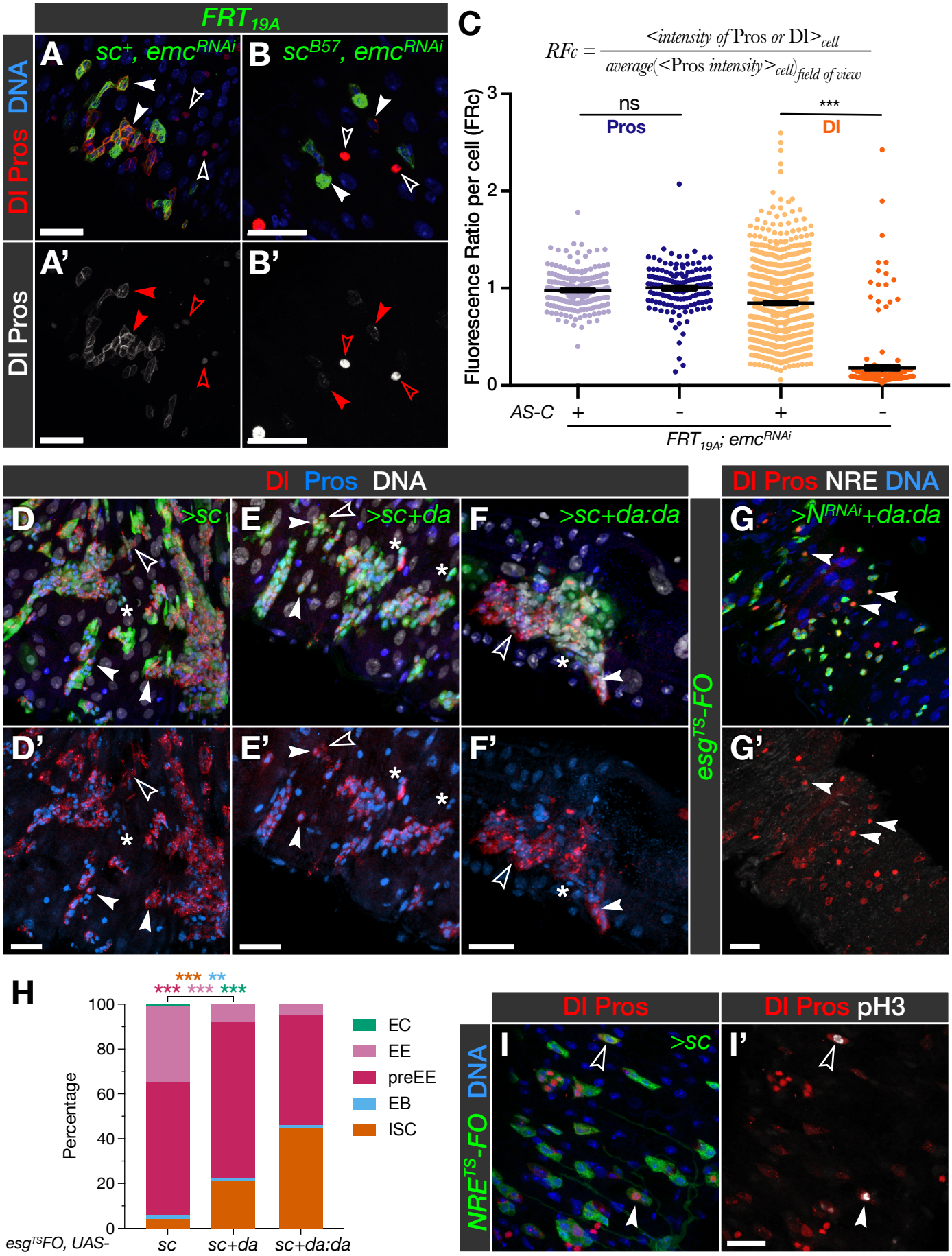

(from the previous page)

Figure 7. Sc:Da and Da:Da antagonise each other in EE formation but collaborate in ISC maintenance.
A-C. Emc antagonises Sc in inducing Dl expression. Loss of the *AS-C* using the sc^{B57} deficiency reduces the increase in Dl expression observed with knockdown of *emc* (B, compare with A). Dl levels are quantified by comparison with those of Pros (see Appendix). Numbers (Dl^+ cells/$Pros^+$ cells) are 210/146 and 718/210 for $UAS\text{-}emc^{RNAi}{}_{NIG}$ and $UAS\text{-}emc^{RNAi}{}_{NIG}$, $Df(1)sc^{B57}$, respectively. P-values are <0.05, <0.01 and <0.001 for one, two or three asterisks (Mann-Whitney test). **D-F.** Antagonism/collaboration between Sc and Da. Solid arrowheads: Dl^+/$Pros^+$ pre-EEs; empty arrowheads: Dl^+ ISCs; asterisks: $Pros^+$ EEs. Overexpression of Sc leads to a dramatic increase of Dl^+/$Pros^+$ pre-EEs and $Pros^+$ EEs, but maintains a population of Dl^+ ISCs (D). The population of ISCs progressively increases by co-expression of monomeric Da (E) and dimeric Da:Da (F), at the cost of EE differentiation (E, F) and pre-EE formation (F). Quantified in H. **G.** Da:Da antagonises EE formation. While reduction of Notch signalling leads to an excess of EEs, simultaneous overexpression of Da:Da and *N*-specific RNAi results in very few $Pros^+$ cells (solid arrowheads, compare with Fig 4A). **H.** Stacked bars plots summarising the cell type composition of $esg^{TS}\text{-}FO$ tissue. Numbers (total GFP^+ cells / fields of view) are 1241/6, 2131/10 and not determined/11 for *UAS-sc, UAS-sc, UAS-da*, and *UAS-sc, UAS-da:da*, respectively. p-values are <0.05, <0.01 and <0.001 for one, two or three asterisks (see Tables S1 and S2). **I.** Sc can induce decommitment of EBs. Expression of Sc with $NRE^{TS}\text{-}FO$ leads to reacquisition of ISC properties (Dl expression, mitosis assessed with phospho-Histone 3, empty arrowhead) and pre-EE formation (Pros expression and mitosis, solid arrowhead). Scale bars: 20μm.

Figure 8

Puig-Barbe et al., 2023

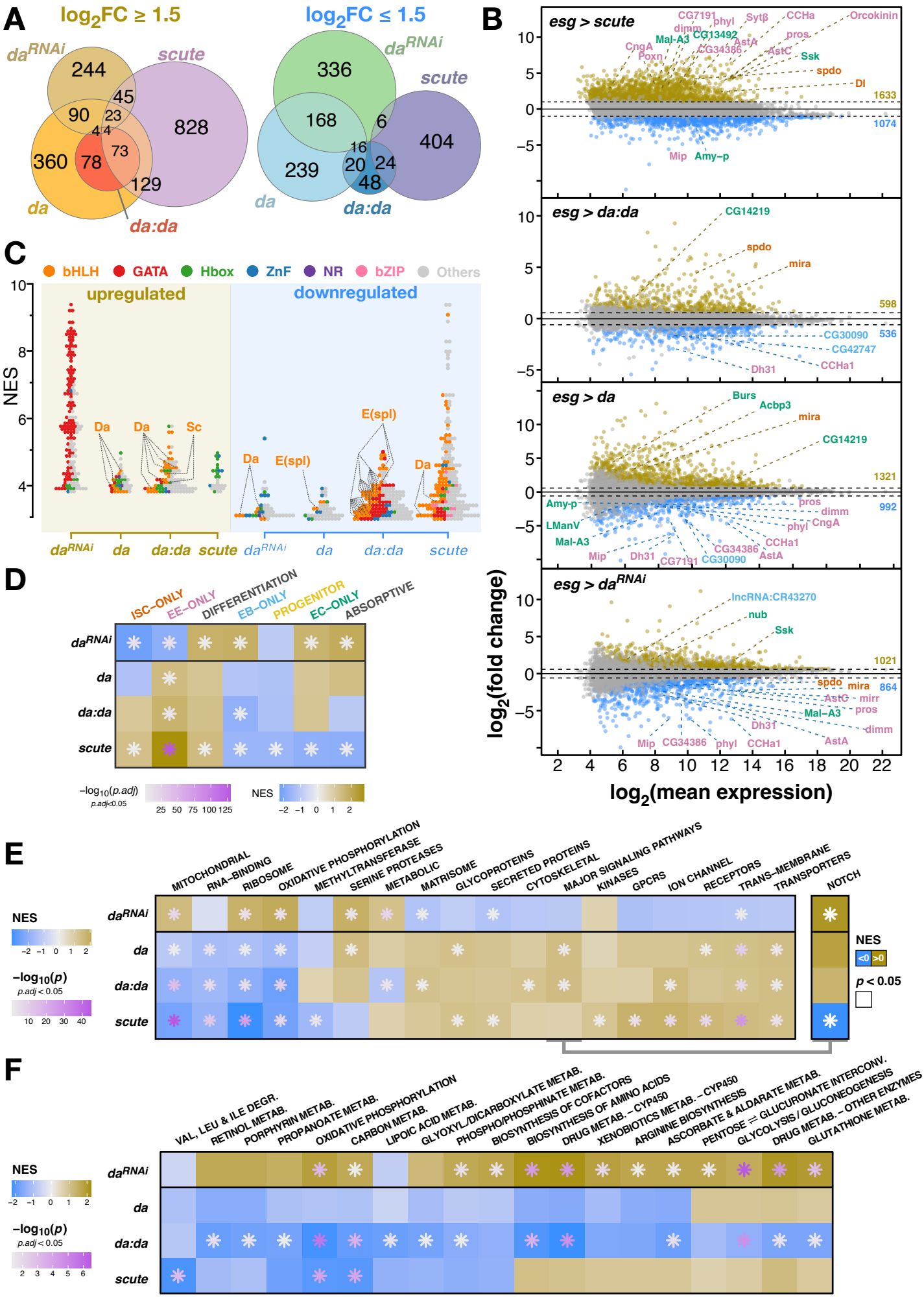

(from the previous page)

Figure 8. Da and Sc cooperate to induce expression of the ISC signature.
A. Euler diagrams showing the intersections of sets of genes either upregulated (left) or downregulated (right) by *da*^{RNAi}, Da:Da, Da and Sc, with fold changes larger than $\log_2(1.5)$. The area of the sets denotes (approximately) the size of the intersection. **B.** MA plots for the overexpression of *da*^{RNAi}, Da:Da, Da and Sc, respectively. Some genes of interest are identified because of their role or expression pattern. Colours match the cell types where genes are expressed. **C**. Beeswarm plots of the normalised enrichment scores of DNA motifs found in upregulated at $\log_2FC \geq 1.5$ (brown, left) or downregulated at $\log_2FC \leq 1.5$ (blue, right) genes in the four conditions analysed, using RcisTarget. Dots represent individual motifs, binned for simplicity of representation, and coloured by the type of transcription factor they are bound by. Those specifically bound by Da, Sc and E(spl) proteins are identified. **D-F**. Heatmaps of gene set enrichment scores for sets of genes that are: expressed in specific cell types (Dutta *et al*, 2015) (D), annotated because of their broad molecular function in *Drosophila* (Hu *et al*, 2015) (E) or belonging to annotated KEGG pathways (F). Asterisks indicate the enrichment scores with significant adjusted p-values, with colour indicating the level of significance. The colourmap of NES scores corresponds to different values in each heatmap.

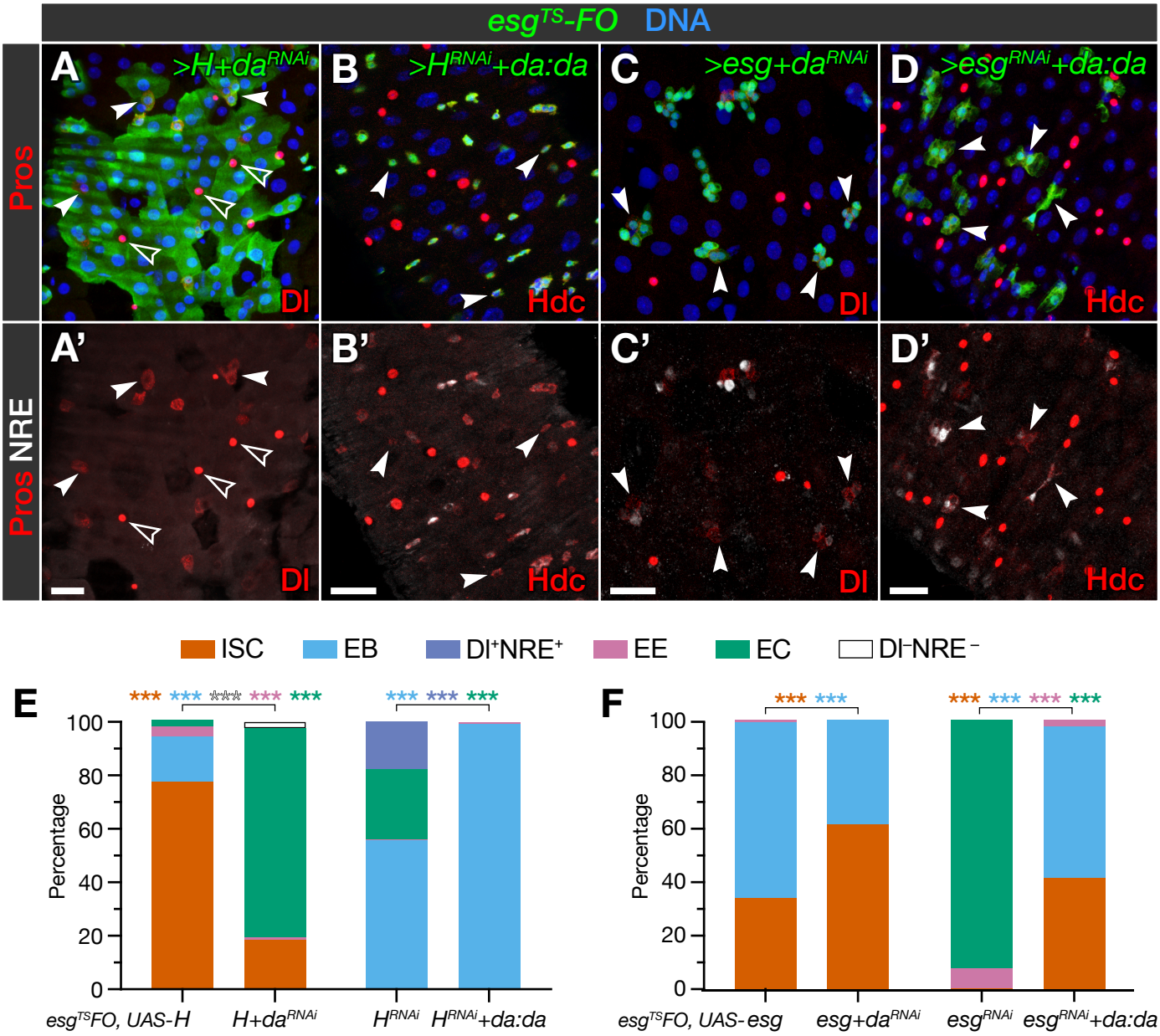

Figure 9. *da* is epistatic to Notch signalling but acts in parallel with *esg*.
Solid arrowheads: ISCs (Hdc⁺/NRE⁻ or Dl⁺/NRE⁻); empty arrowheads: EEs (Pros⁺). **A-B.** *da* is epistatic over Notch signalling. Loss of *da* leads to EC and EE differentiation when Notch signalling is impaired by overexpression of *H* (A), while overexpression of *da:da* maintains cell undifferentiated even when Notch signalling is exacerbated by knockdown of *H* (B). **C-D.** *da* and *esg* function in parallel to prevent differentiation. Overexpression of *esg* can prevent differentiation and compensate for the loss of *da* (C), while overexpression of *da:da* can similarly compensate for the loss of *esg*, including prevention of EE formation (D). **E-F.** Stacked bars plots summarising the cell type composition of *esg^{TS}-FO* tissue. Numbers (total GFP⁺ cells / fields of view) are 1510/21, 1810/21, 613/8 and 984/15 for *UAS-H*, *UAS-H+UAS-da$^{RNAi}_{JF}$*, *UAS-H$^{RNAi}_{HMS}$* and *UAS-H$^{RNAi}_{HMS}$+UAS-da:da*, respectively (E) and 850/9, 1236/12, 628/18 and 939/19 for for *UAS-esg UAS-esg+UAS-da$^{RNAi}_{JF}$*, *UAS-esg$^{RNAi}_{HMS}$* and *UAS-esg$^{RNAi}_{HMS}$+UAS-da:da*, respectively (F). p-values are <0.05, <0.01 and <0.001 for one, two or three asterisks (see Tables S1 and S2 for further details). Scale bars: 20μm.

Figure 10 Puig-Barbe et al., 2023

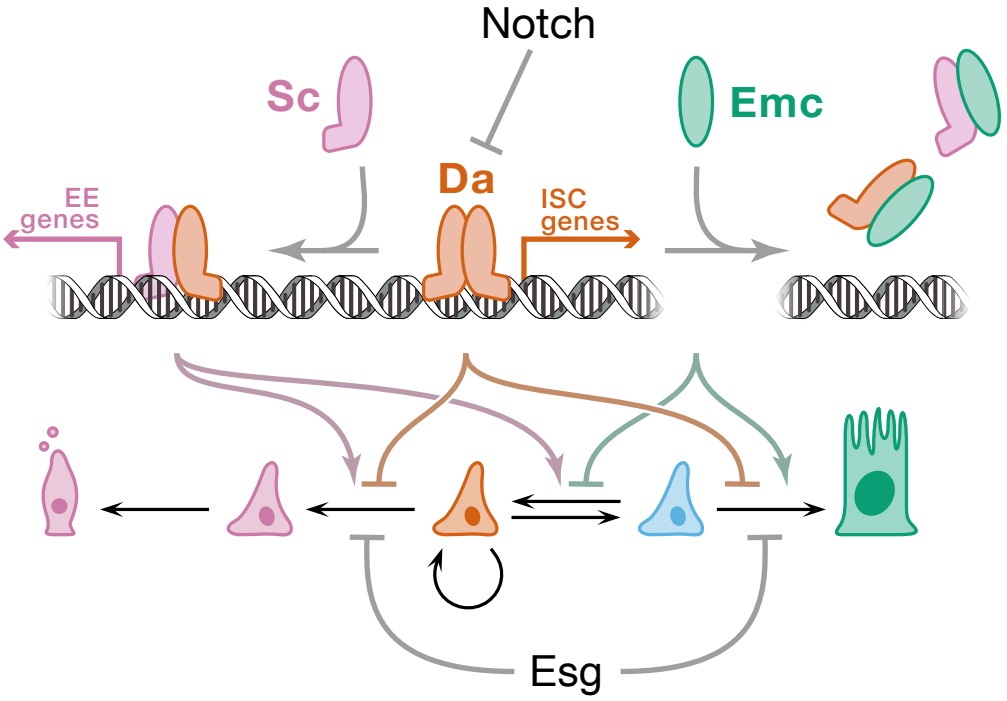

Fig 10. Sc, Da and Emc regulate self-renewal and differentiation in the intestine.
Orange arrows: Da homodimers maintain ISCs and EBs undifferentiated, antagonising EC differentiation and pre-EE formation by inducing expression of ISC-specific genes. Pink arrows: An increase of Sc expression induces formation of Da:Sc heterodimers, which steer the transcriptional program towards pre-EE formation; Sc can also induce expression of the ISC-specific signature, potentially leading to EB decommitment if its activity is not prevented by titration by Emc. Green arrows: Emc increased expression in EBs maintains commitment for EC differentiation and can direct terminal EC differentiation by interruption of Da:Da and Da:Sc transcriptional activities. This occurs in parallel to Esg prevention of differentiation and Notch signalling being upstream and opposing Da:Da to induce EC differentiation.

Table 1. Summary statistics of bHLH-bound motif enrichment.

Gene set	bHLH / total enriched motifs	Max rank NES	Median rank NES	Genes with enriched bHLH motifs / set size
UAS-da:da, upregulated	28 / 98	3	25	118 / 220
UAS-da, upregulated	11 / 44	3	33	248 / 628
UAS-da^{RNAi}, downregulated	7 / 43	13	28	106 / 382

NES, normalised enrichment score. Max, maximum